

Supplementary information

New Marine-Derived Indolymethyl Pyrazinoquinazoline Alkaloids with Promising Antimicrobial Profiles

*Solida Long^a, Diana I. S. P. Resende^{a,b}, Andreia Palmeira^{a,b}, Anake Kijjoa^{b,c}, Artur M. S. Silva^d,
Maria Elizabeth Tiritan^{a,b,e}, Patrícia Pereira-Terra^{b,c}, Joana Freitas-Silva^{b,c}, Sandra Barreiro^f,
Renata Silva^f, Fernando Remião^f, Eugénia Pinto^{b,g}, Paulo Martins da Costa^{b,c*}, Emília Sousa^{a,b*},
and Madalena M. M. Pinto^{a,b}*

^aLQOF - Laboratório de Química Orgânica e Farmacêutica, Departamento de Ciências Químicas, Faculdade de Farmácia, Universidade do Porto, Rua de Jorge Viterbo Ferreira, 228, 4050-313 Porto, Portugal;

^bCIIMAR - Centro Interdisciplinar de Investigação Marinha e Ambiental, Terminal de Cruzeiros do Porto de Leixões, Av. General Norton de Matos S/N, 4450-208 Matosinhos, Portugal;

^cICBAS - Instituto de Ciências Biomédicas Abel Salazar, Universidade do Porto, Rua de Jorge Viterbo Ferreira, 228, 4050-313 Porto, Portugal;

^dQOPNA - Química Orgânica, Produtos Naturais e Agroalimentares, Departamento de Química, Universidade de Aveiro, 3810-193 Aveiro, Portugal;

^eCESPU, Instituto de Investigação e Formação Avançada em Ciências e Tecnologias da Saúde (IINFACETS), Rua Central de Gandra, 1317, 4585-116 Gandra PRD, Portugal;

^fUCIBIO-REQUIMTE, Laboratório de Toxicologia, Departamento de Ciências Biológicas, Faculdade de Farmácia, Universidade do Porto, Rua de Jorge Viterbo Ferreira, 228, 4050-313 Porto, Portugal;

^gLaboratório de Microbiologia, Departamento de Ciências Biológicas, Faculdade de Farmácia, Universidade do Porto, Rua de Jorge Viterbo Ferreira, 228, 4050-313 Porto, Portugal

*Corresponding authors: esousa@ff.up.pt, pmcosta@icbas.up.pt

Contents

1. NMR Spectra.....	2
2. Enantioselective liquid chromatography.....	19
2.1 Chiral analysis of compounds 22-32.....	19
2.2 Enantioselective liquid chromatography separation of compounds 22, 23, and 26.....	24
3. High resolution mass spectra.....	26
4. Antimicrobial activity.....	32

1. NMR Spectra

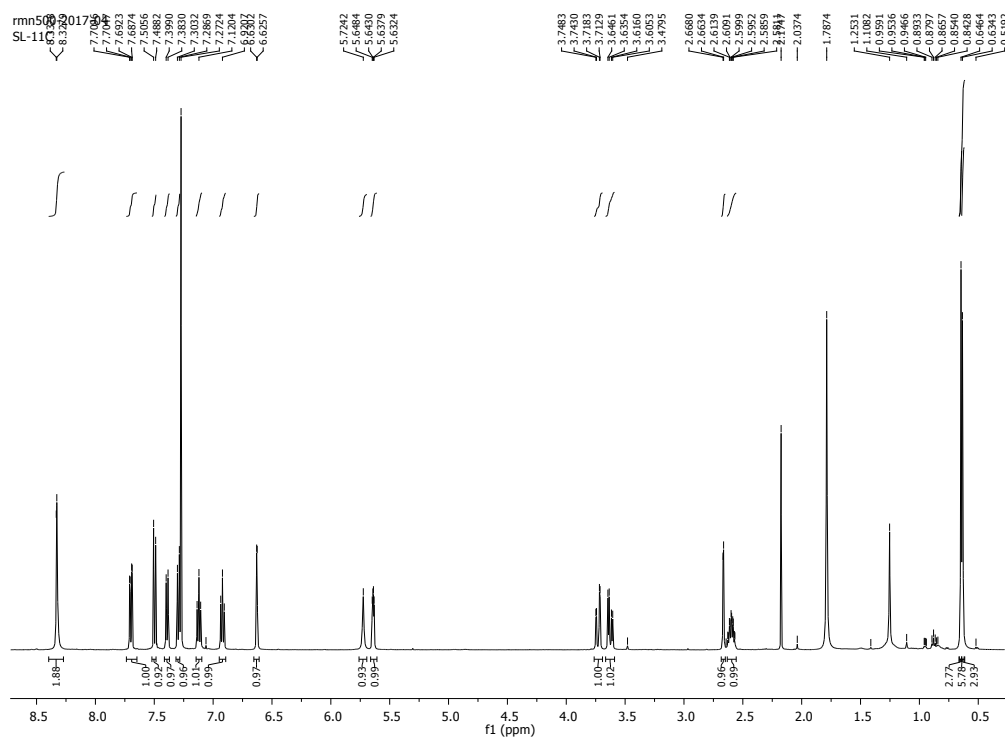


Fig. S1. ^1H NMR spectrum of (1*S*,4*R*)-4-((1*H*-indol-3-yl)methyl)-8-chloro-1-isopropyl-1,2-dihydro-6*H*-pyrazino[2,1-*b*]quinazoline-3,6(4*H*)-dione (**22**) (CDCl_3 , 300, MHz).

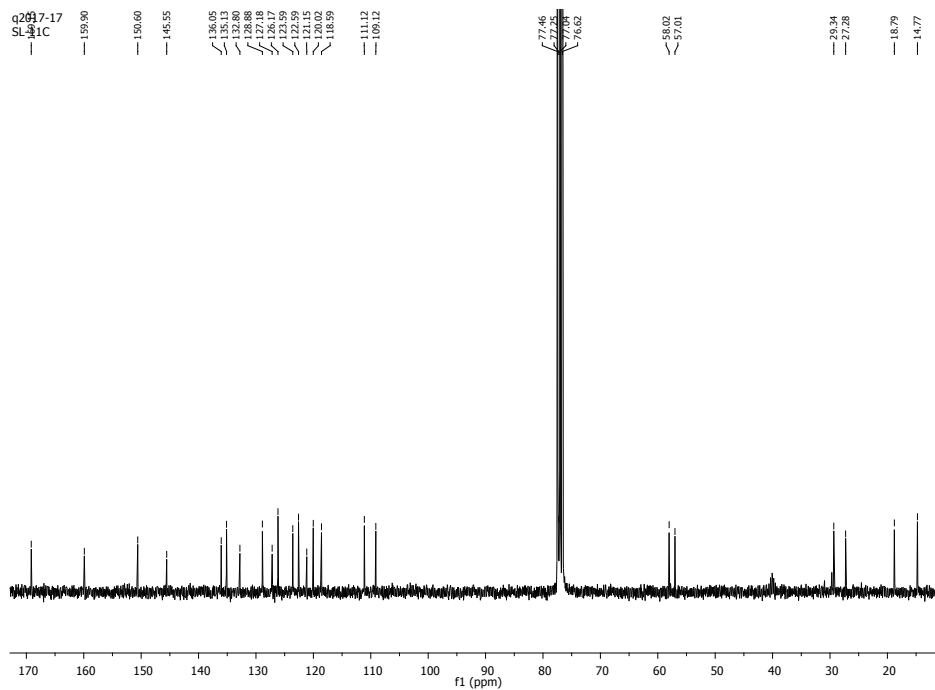


Fig. S2. ^{13}C NMR spectrum of (1*S*,4*R*)-4-((1*H*-indol-3-yl)methyl)-8-chloro-1-isopropyl-1,2-dihydro-6*H*-pyrazino[2,1-*b*]quinazoline-3,6(4*H*)-dione (**22**) (CDCl_3 , 75, MHz).

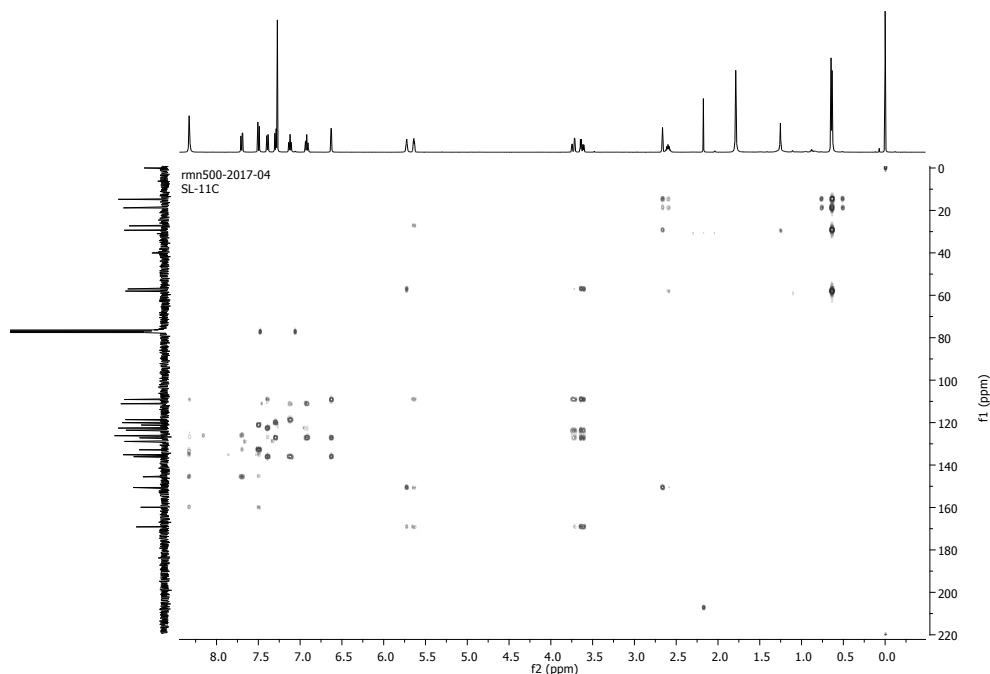


Fig. S3. ^1H NMR spectrum of (1*S*,4*R*)-4-((1*H*-indol-3-yl)methyl)-8-chloro-1-isopropyl-1,2-dihydro-6*H*-pyrazino[2,1-*b*]quinazoline-3,6(4*H*)-dione (**22**) (CDCl_3 , 300, MHz).

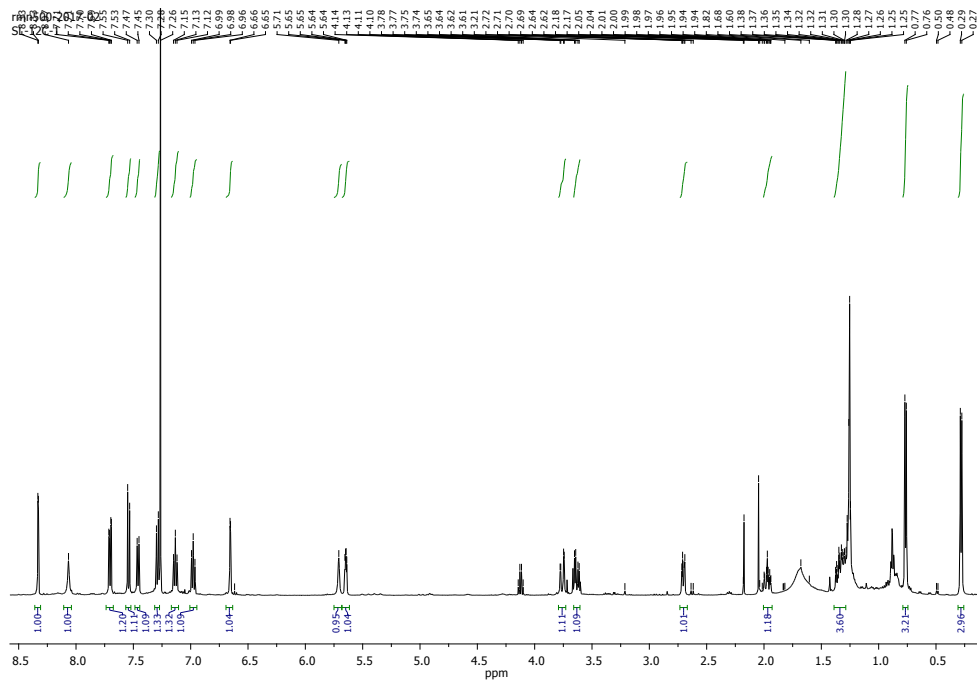


Fig. S4. ^1H NMR spectrum of (1*S*,4*R*)-4-((1*H*-indol-3-yl)methyl)-8-chloro-1-isobutyl-1,2-dihydro-6*H*-pyrazino[2,1-*b*]quinazoline-3,6(4*H*)-dione (**23**) (CDCl_3 , 300, MHz).

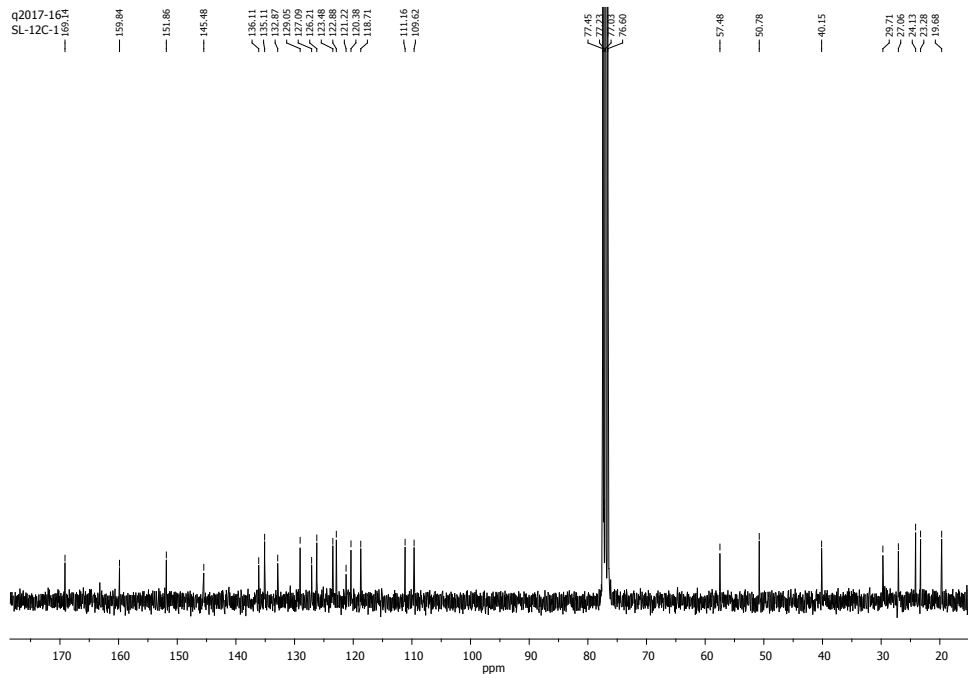


Fig. S5. ^{13}C NMR spectrum of (1*S*,4*R*)-4-((1*H*-indol-3-yl)methyl)-8-chloro-1-isobutyl-1,2-dihydro-6*H*-pyrazino[2,1-*b*]quinazoline-3,6(4*H*)-dione (**23**) (CDCl_3 , 75, MHz).

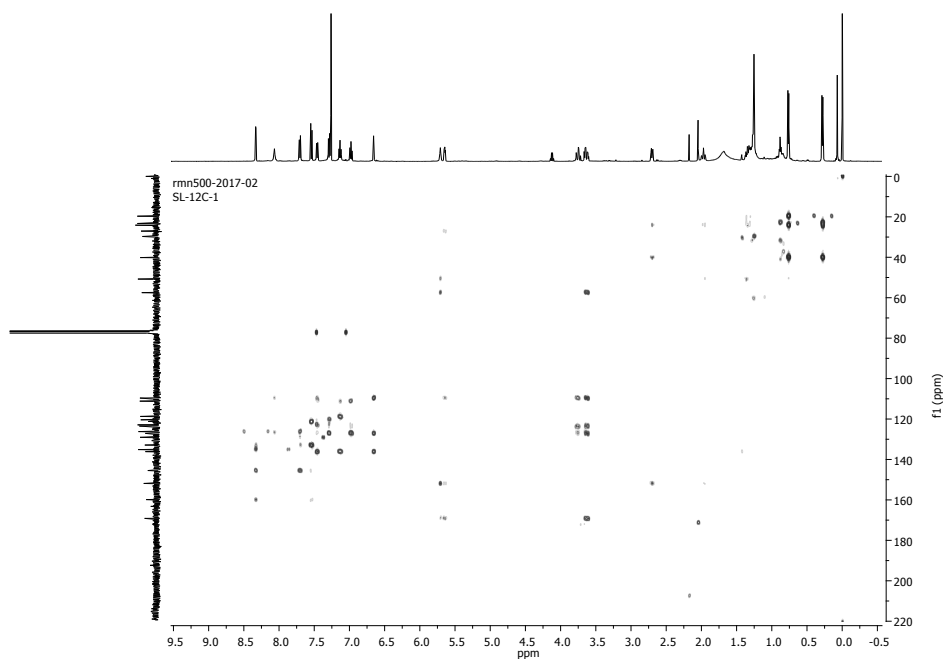


Fig. S6. HMBC NMR spectrum of (1*S*,4*R*)-4-((1*H*-indol-3-yl)methyl)-8-chloro-1-isobutyl-1,2-dihydro-6*H*-pyrazino[2,1-*b*]quinazoline-3,6(4*H*)-dione (**23**) (CDCl_3 , 300, MHz).

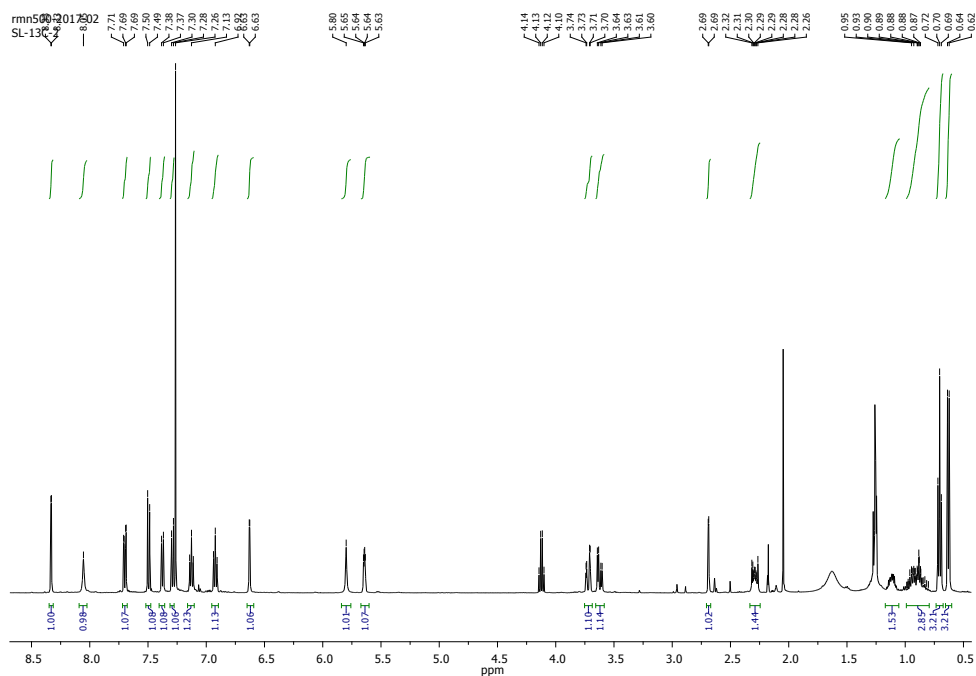


Fig. S7. ^1H NMR spectrum of (1*S*,4*R*)-4-((1*H*-indol-3-yl)methyl)-1-((*S*)-sec-butyl)-8-chloro-1,2-dihydro-6*H*-pyrazino[2,1-*b*]quinazoline-3,6(4*H*)-dione (**24**) (CDCl_3 , 300, MHz).

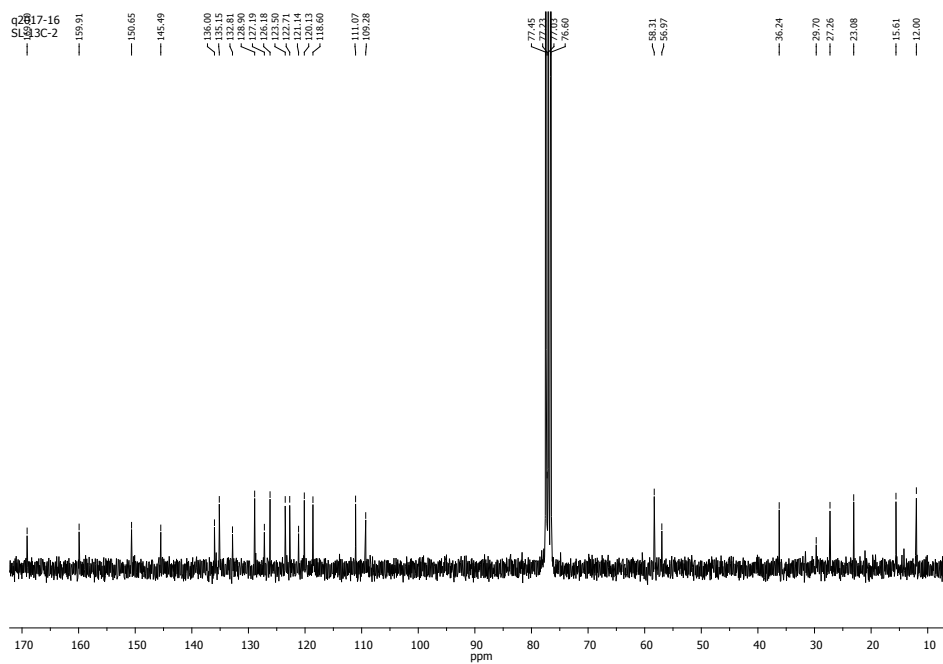


Fig. S8. ^{13}C NMR spectrum of (1*S*,4*R*)-4-((1*H*-indol-3-yl)methyl)-1-((*S*)-sec-butyl)-8-chloro-1,2-dihydro-6*H*-pyrazino[2,1-*b*]quinazoline-3,6(4*H*)-dione (**24**) (CDCl_3 , 75, MHz).

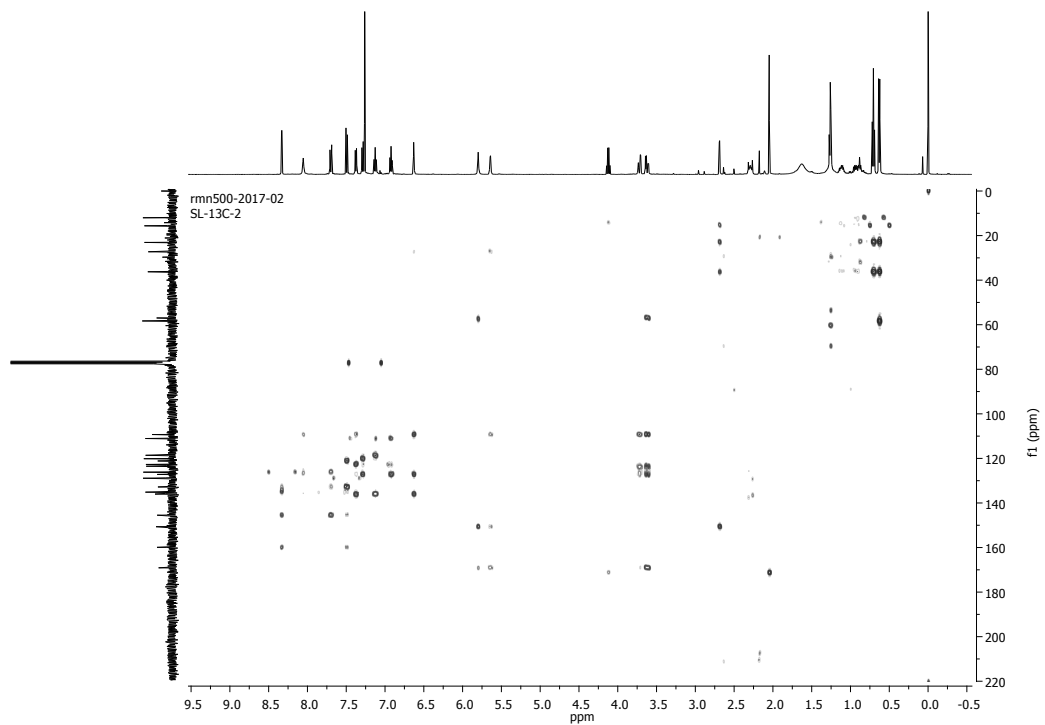


Fig. S9. HMBC NMR spectrum of (1*S*,4*R*)-4-((1*H*-indol-3-yl)methyl)-1-((*S*)-sec-butyl)-8-chloro-1,2-dihydro-6*H*-pyrazino[2,1-*b*]quinazoline-3,6(4*H*)-dione (**24**) (CDCl₃, 300, MHz).

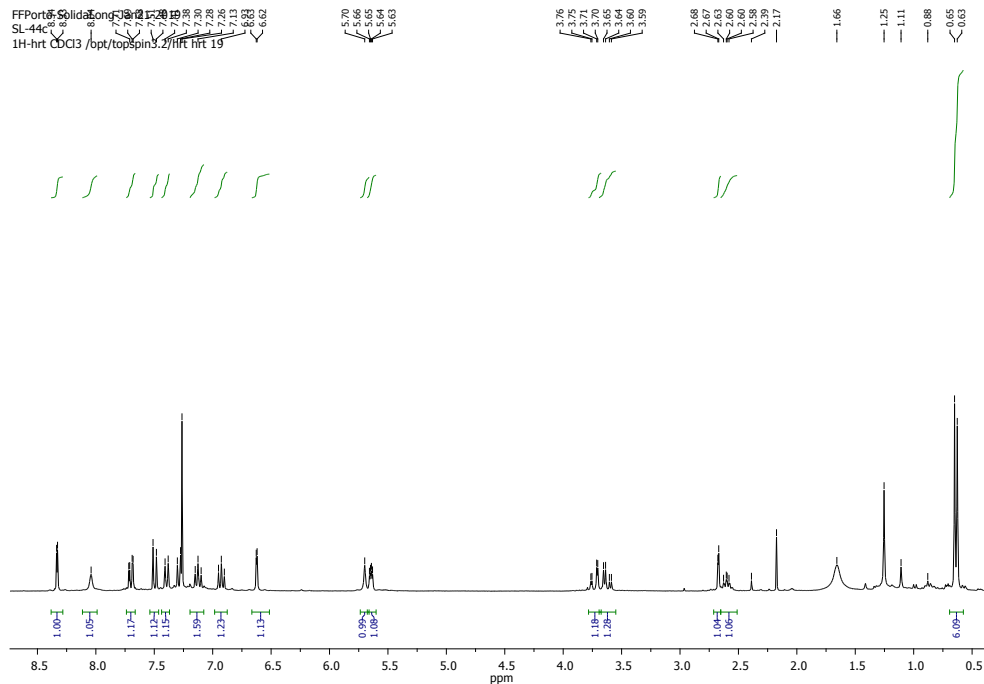


Fig. S10. ¹H NMR spectrum of (1*S*,4*R*)-4-((1*H*-indol-3-yl)methyl)-8,10-dichloro-1-isopropyl-1,2-dihydro-6*H*-pyrazino[2,1-*b*]quinazoline-3,6(4*H*)-dione (**25**) (CDCl₃, 300, MHz).

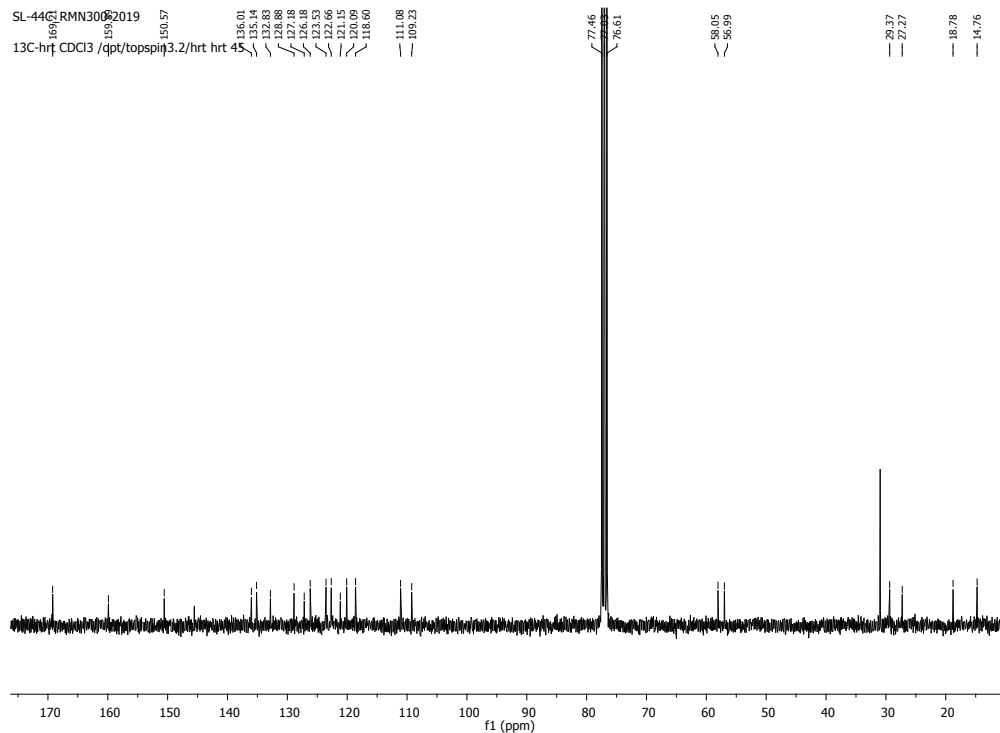


Fig. S11. ^{13}C NMR spectrum of (1*S*,4*R*)-4-((1*H*-indol-3-yl)methyl)-8,10-dichloro-1-isopropyl-1,2-dihydro-6*H*-pyrazino[2,1-*b*]quinazoline-3,6(4*H*)-dione (**25**) (CDCl_3 , 75, MHz).

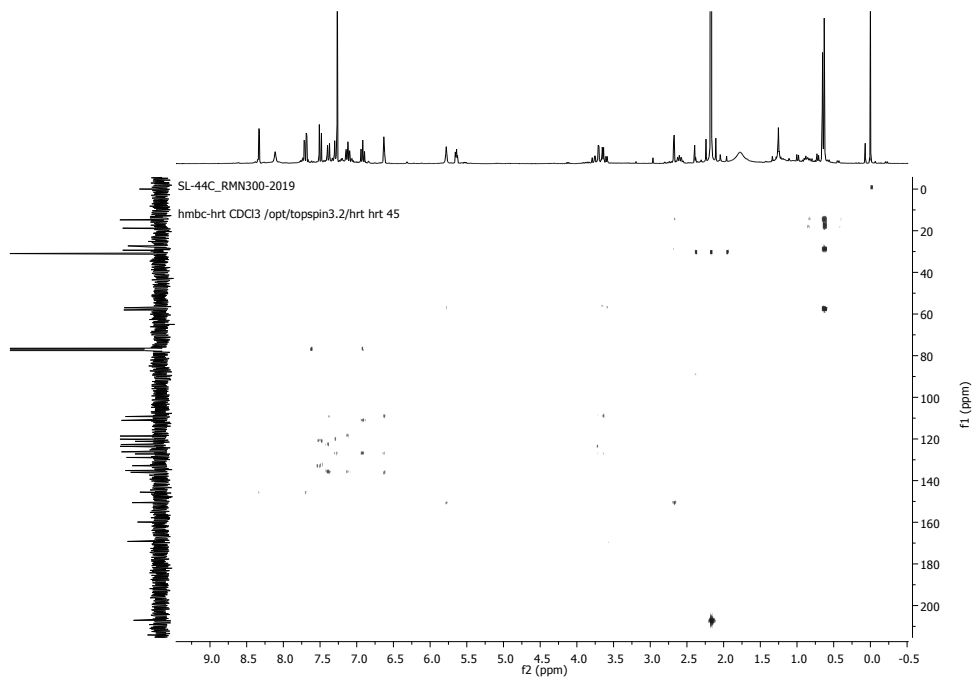


Fig. S12. HRMS NMR spectrum of (1*S*,4*R*)-4-((1*H*-indol-3-yl)methyl)-8,10-dichloro-1-isopropyl-1,2-dihydro-6*H*-pyrazino[2,1-*b*]quinazoline-3,6(4*H*)-dione (**25**) (CDCl_3 , 300, MHz).

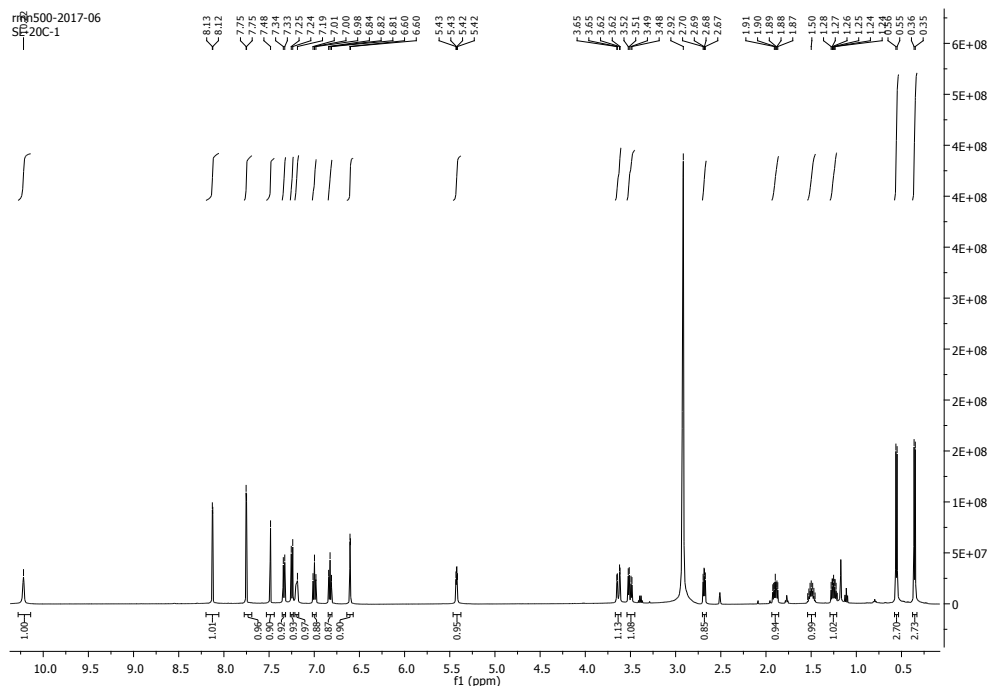


Fig. S13. ¹H NMR NMR spectrum of (1*S*,4*R*)-4-((1*H*-indol-3-yl)methyl)-8,10-dichloro-1-isobutyl-1,2-dihydro-6*H*-pyrazino[2,1-*b*]quinazoline-3,6(4*H*)-dione (**26**) (DMSO-*d*₆, 300, MHz).

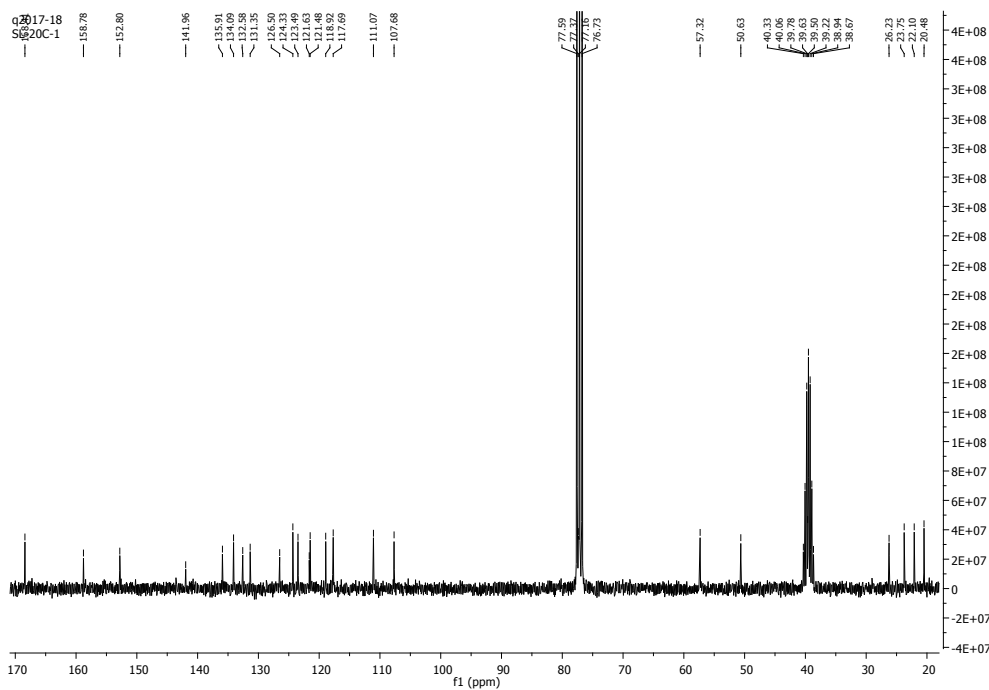


Fig. S14. ¹³C NMR NMR spectrum of (1*S*,4*R*)-4-((1*H*-indol-3-yl)methyl)-8,10-dichloro-1-isobutyl-1,2-dihydro-6*H*-pyrazino[2,1-*b*]quinazoline-3,6(4*H*)-dione (**26**) (DMSO-*d*₆, 75, MHz).

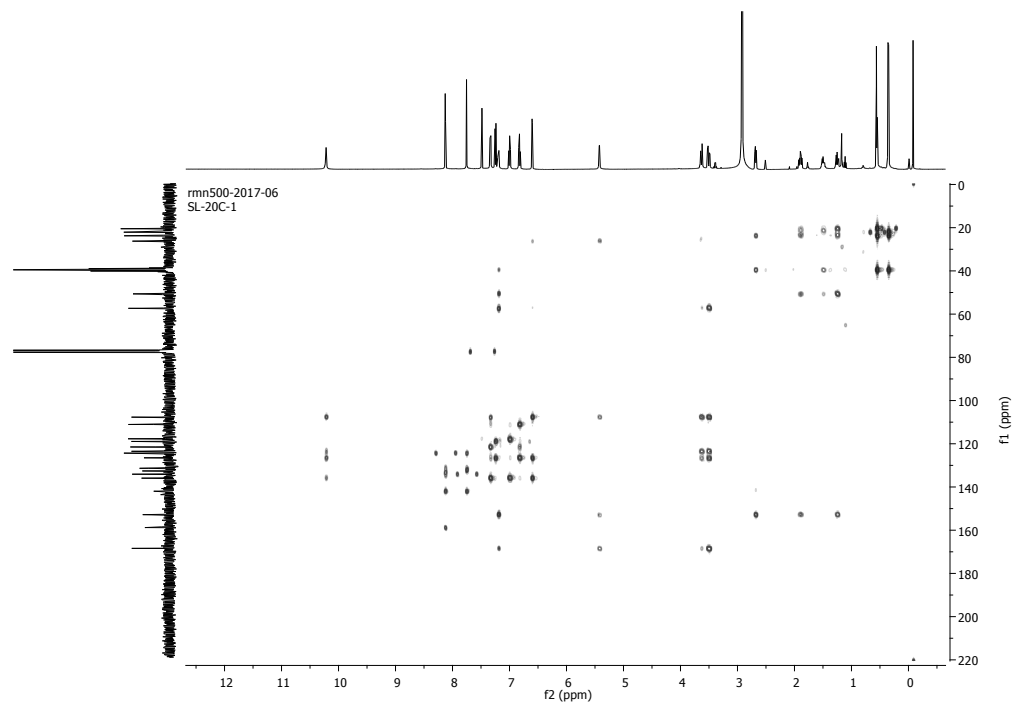


Fig. S15. HMBC NMR spectrum of (1*S*,4*R*)-4-((1*H*-indol-3-yl)methyl)-8,10-dichloro-1-isobutyl-1,2-dihydro-6*H*-pyrazino[2,1-*b*]quinazoline-3,6(4*H*)-dione (**26**) (DMSO-*d*₆, 300, MHz)

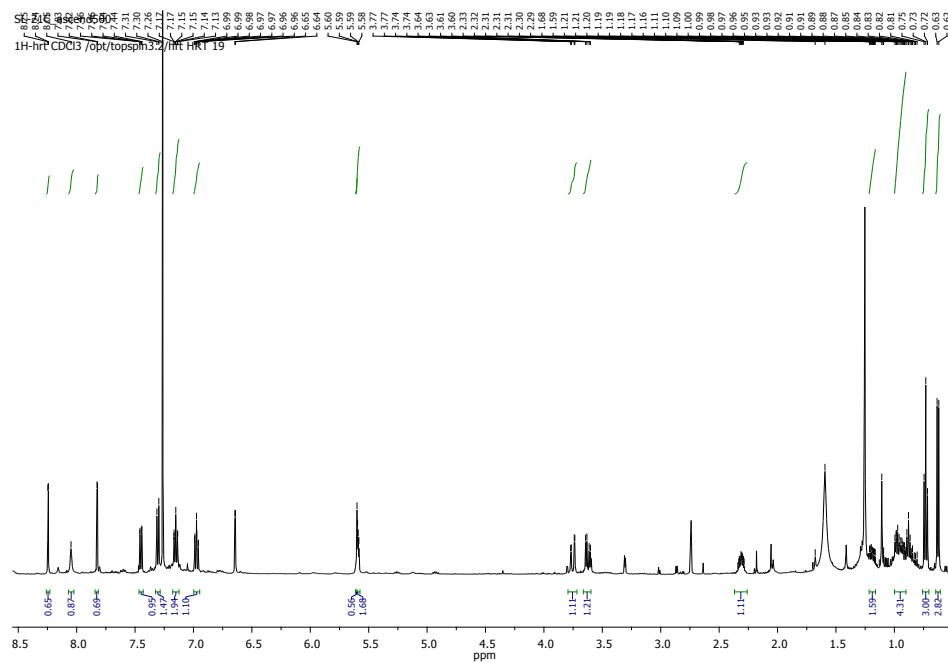


Fig. S16. ¹H NMR spectrum of (1*S*,4*R*)-4-((1*H*-indol-3-yl)methyl)-1-((*S*)-sec-butyl)-8,10-dichloro-1,2-dihydro-6*H*-pyrazino[2,1-*b*]quinazoline-3,6(4*H*)-dione (**27**) (CDCl₃, 300, MHz).

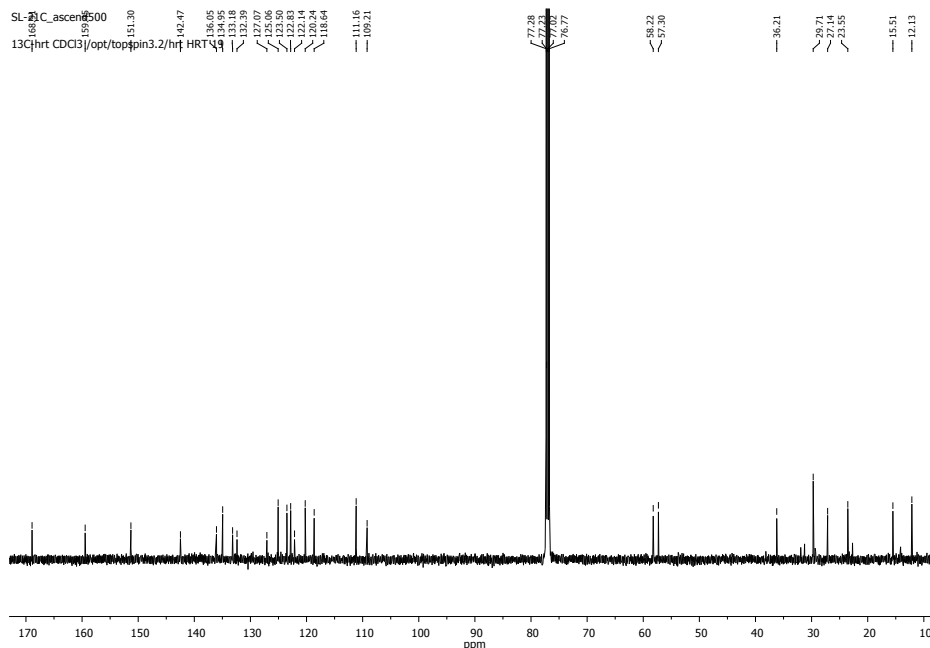


Fig. S17. ^{13}C NMR spectrum of (1*S*,4*R*)-4-((1*H*-indol-3-yl)methyl)-1-((*S*)-sec-butyl)-8,10-dichloro-1,2-dihydro-6*H*-pyrazino[2,1-*b*]quinazoline-3,6(4*H*)-dione (**27**) (CDCl_3 , 75, MHz).

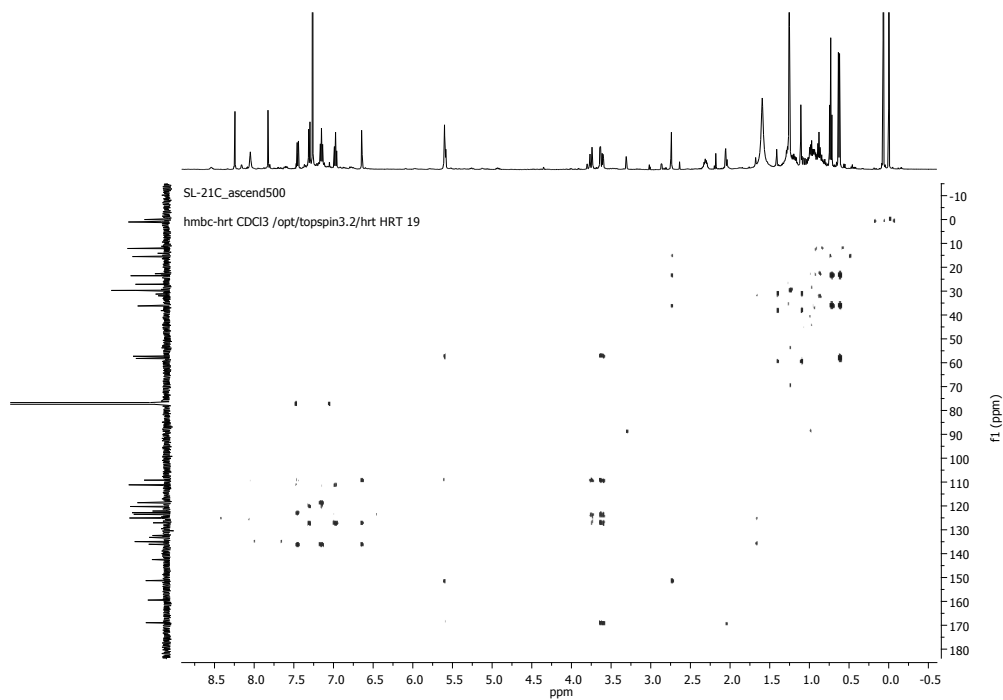


Fig. S18. HMBC spectrum of (1*S*,4*R*)-4-((1*H*-indol-3-yl)methyl)-1-((*S*)-sec-butyl)-8,10-dichloro-1,2-dihydro-6*H*-pyrazino[2,1-*b*]quinazoline-3,6(4*H*)-dione (**27**) (CDCl_3 , 300, MHz).

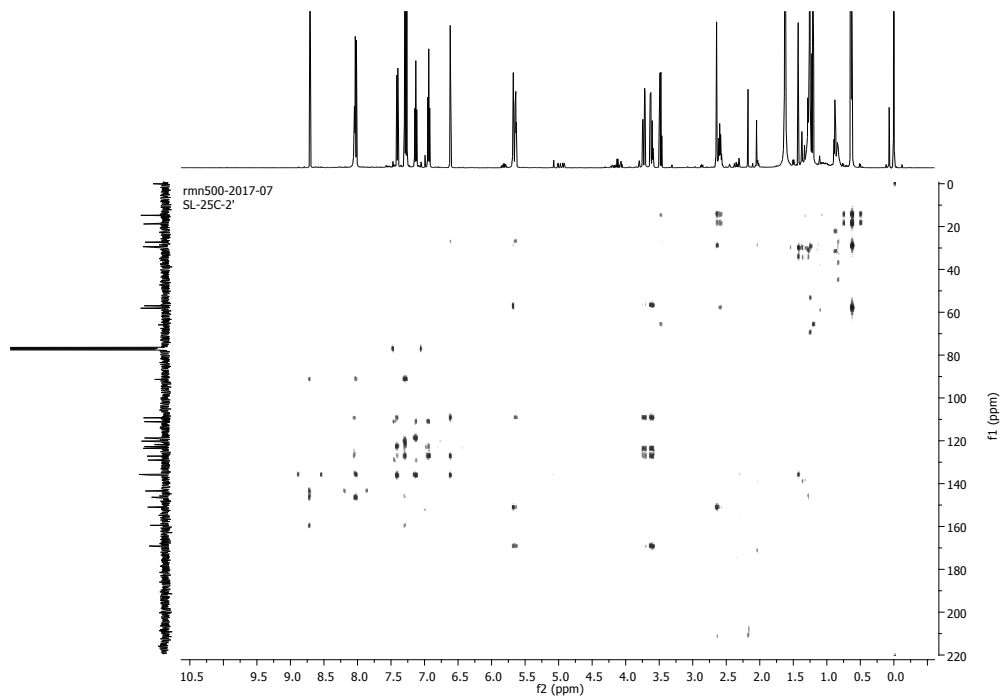


Fig. S21. HMBC spectrum of (1*S*,4*R*)-4-((1*H*-indol-3-yl)methyl)-8-iodo-1-isopropyl-1,2-dihydro-6*H*-pyrazino[2,1-*b*]quinazoline-3,6(4*H*)-dione (**28**) (CDCl₃, 300, MHz).

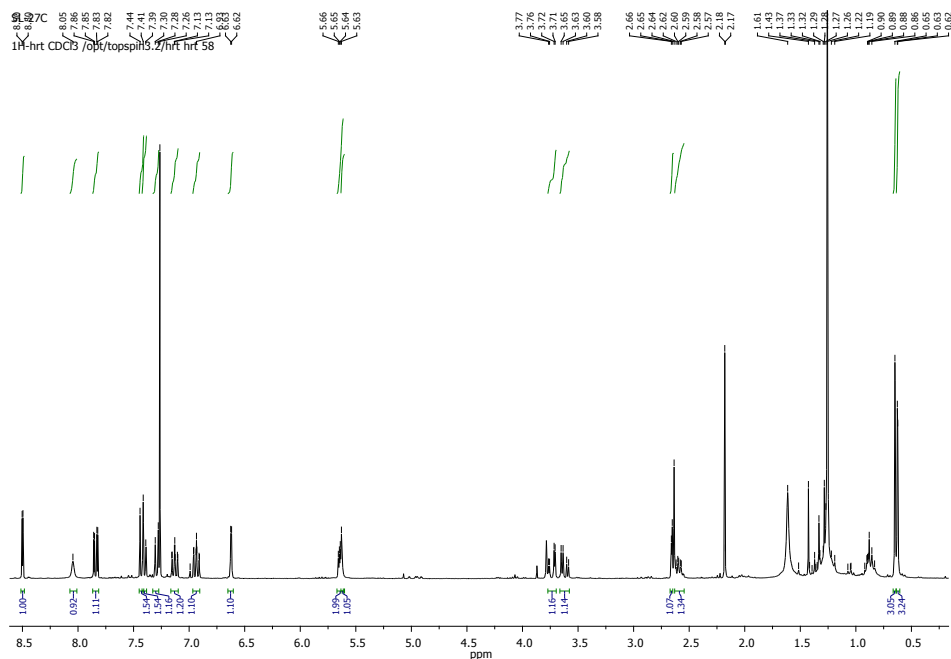


Fig. S22. ¹H NMR spectrum of (1*S*,4*R*)-4-((1*H*-indol-3-yl)methyl)-8-bromo-1-isopropyl-1,2-dihydro-6*H*-pyrazino[2,1-*b*]quinazoline-3,6(4*H*)-dione (**29**) (CDCl₃, 300, MHz).

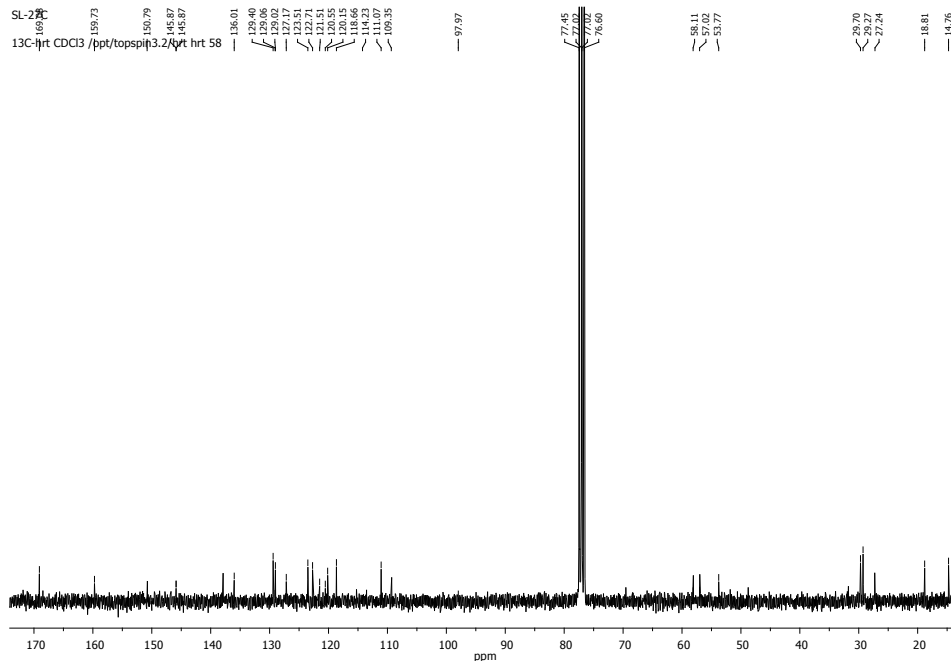


Fig. S23. ^{13}C NMR spectrum of (1*S*,4*R*)-4-((1*H*-indol-3-yl)methyl)-8-bromo-1-isopropyl-1,2-dihydro-6*H*-pyrazino[2,1-*b*]quinazoline-3,6(4*H*)-dione (**29**) (CDCl_3 , 75, MHz).

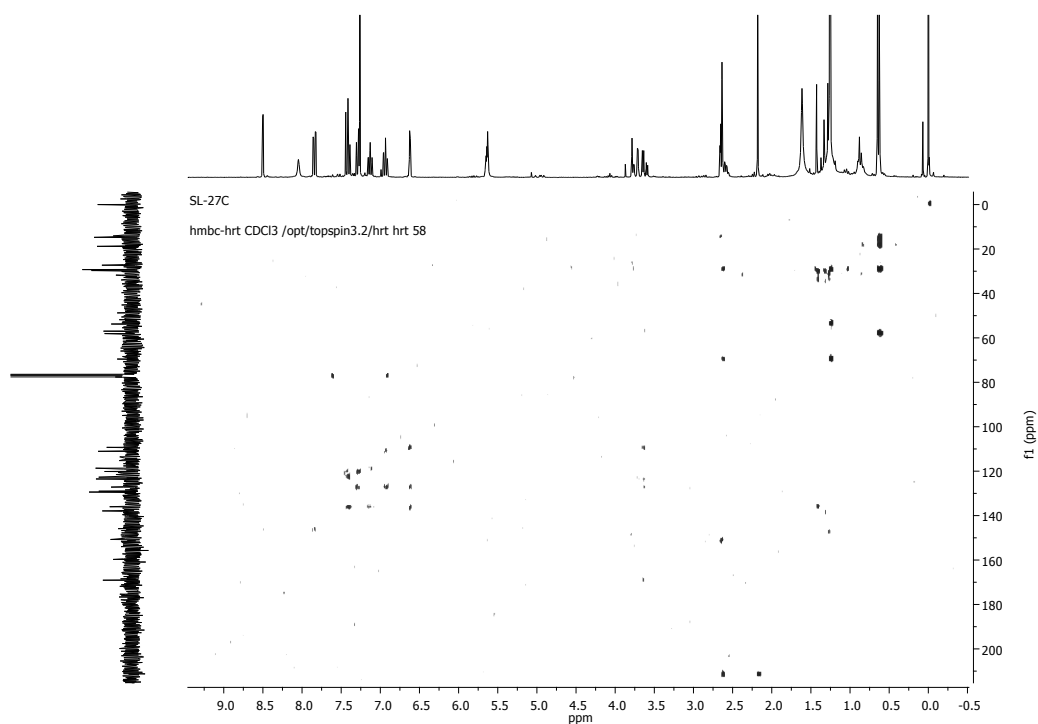


Fig. S24. HMBC spectrum of (1*S*,4*R*)-4-((1*H*-indol-3-yl)methyl)-8-bromo-1-isopropyl-1,2-dihydro-6*H*-pyrazino[2,1-*b*]quinazoline-3,6(4*H*)-dione (**29**) (CDCl_3 , 300, MHz).

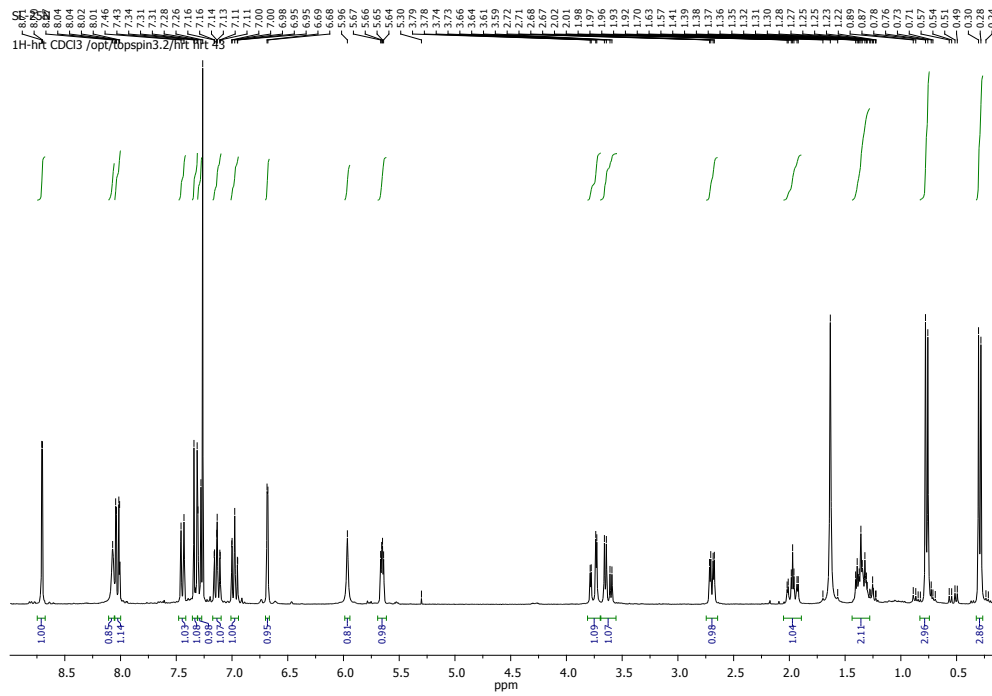


Fig. S25. ¹H NMR spectrum of (1*S*,4*R*)-4-((1*H*-indol-3-yl)methyl)-8-iodo-1-isobutyl-1,2-dihydro-6*H*-pyrazino[2,1-*b*]quinazoline-3,6(4*H*)-dione (**30**) (CDCl₃, 300, MHz).

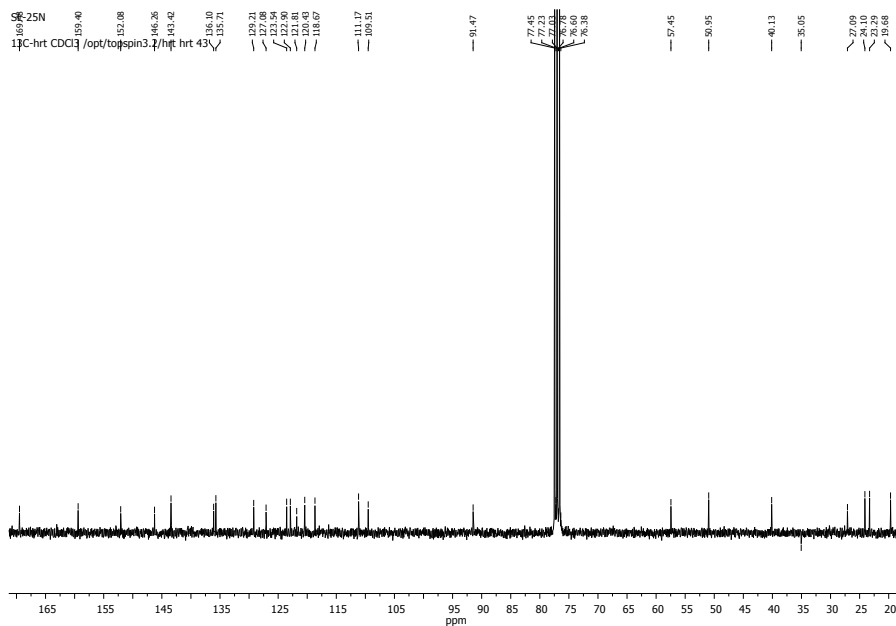


Fig. S26. ¹³C NMR spectrum of (1*S*,4*R*)-4-((1*H*-indol-3-yl)methyl)-8-iodo-1-isobutyl-1,2-dihydro-6*H*-pyrazino[2,1-*b*]quinazoline-3,6(4*H*)-dione (**30**) (CDCl₃, 75, MHz).

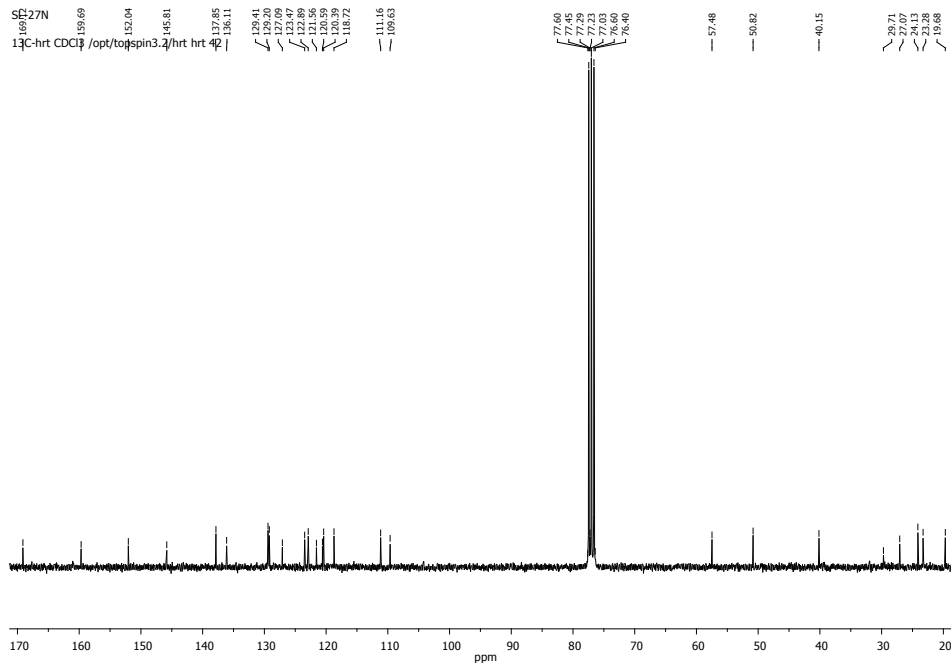


Fig. S29. ¹³C NMR spectrum of (1*S*,4*R*)-4-((1*H*-indol-3-yl)methyl)-8-bromo-1-isobutyl-1,2-dihydro-6*H*-pyrazino[2,1-*b*]quinazoline-3,6(4*H*)-dione (**31**) (CDCl₃, 75, MHz).

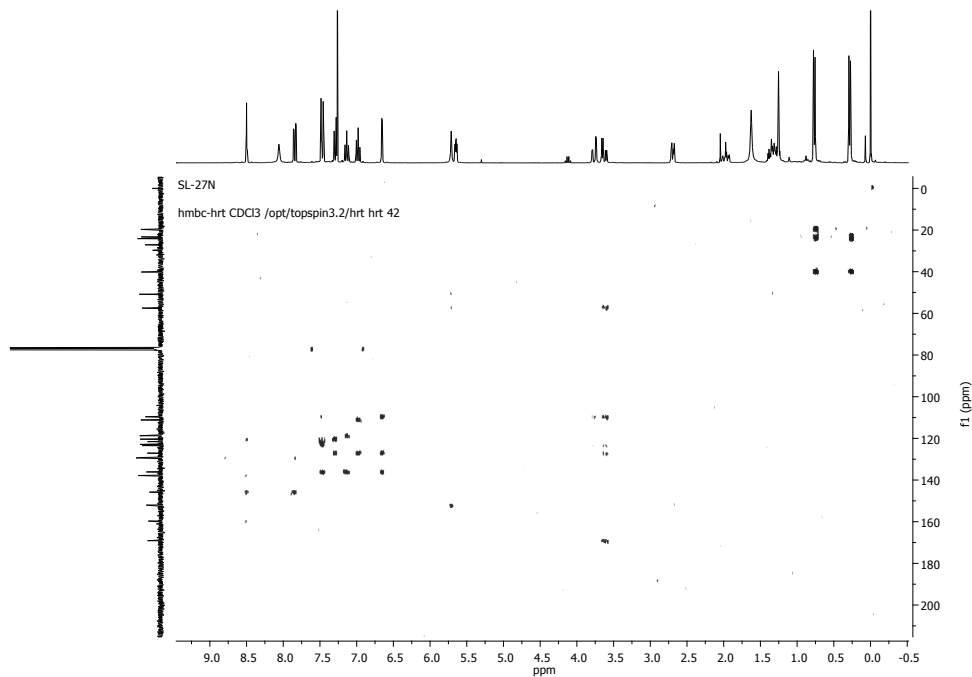


Fig. S30. ¹H NMR spectrum of (1*S*,4*R*)-4-((1*H*-indol-3-yl)methyl)-8-bromo-1-isobutyl-1,2-dihydro-6*H*-pyrazino[2,1-*b*]quinazoline-3,6(4*H*)-dione (**31**) (DMSO-*d*₆, 300, MHz).

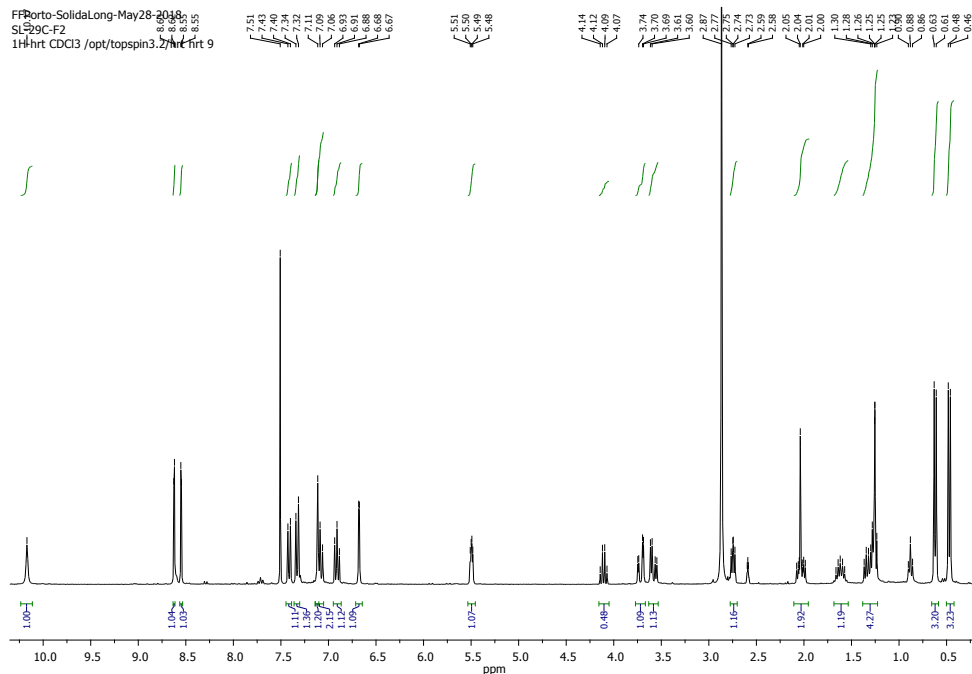


Fig. S31. ^1H NMR spectrum of (1*S*,4*R*)-4-((1*H*-indol-3-yl)methyl)-8,10-diiodo-1-isobutyl-1,2-dihydro-6*H*-pyrazino[2,1-*b*]quinazoline-3,6(4*H*)-dione (**32**) (DMSO- d_6 , 300, MHz).

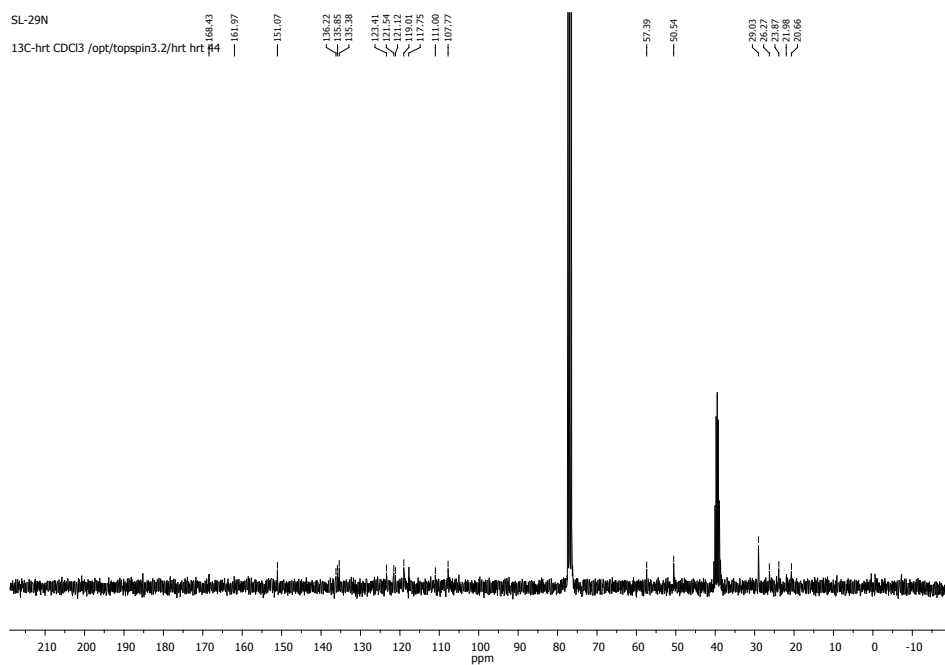


Fig. S32. ^{13}C NMR spectrum of (1*S*,4*R*)-4-((1*H*-indol-3-yl)methyl)-8,10-diiodo-1-isobutyl-1,2-dihydro-6*H*-pyrazino[2,1-*b*]quinazoline-3,6(4*H*)-dione (**32**) (DMSO- d_6 , 75, MHz).

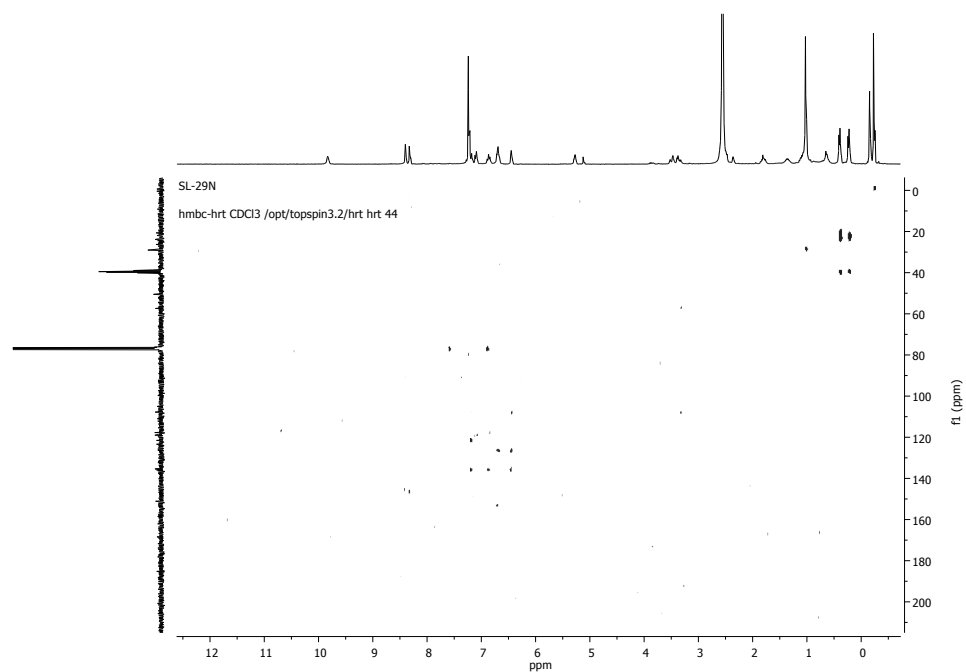


Fig. S33. HMBC spectrum of (1*S*,4*R*)-4-((1*H*-indol-3-yl)methyl)-8,10-diiodo-1-isobutyl-1,2-dihydro-6*H*-pyrazino[2,1-*b*]quinazoline-3,6(4*H*)-dione (**32**) (DMSO-*d*₆, 300, MHz).

2. Enantioselective liquid chromatography

2.1 Chiral analysis of compounds 22-32

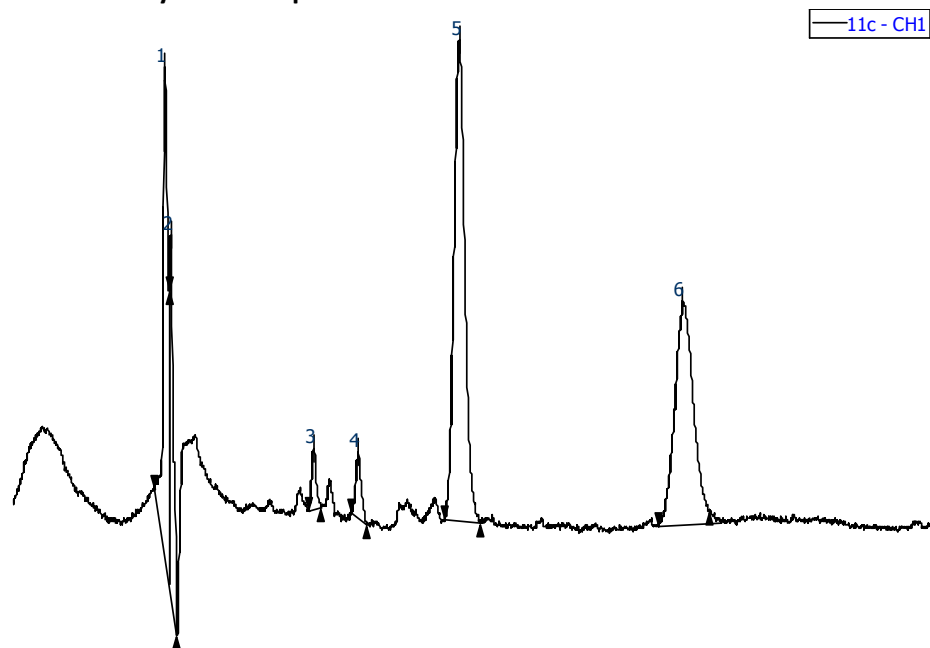


Fig. S34. Chiral analysis of (1*S*,4*R*)-4-((1*H*-indol-3-yl)methyl)-8-chloro-1-isopropyl-1,2-dihydro-6*H*-pyrazino[2,1-*b*]quinazoline-3,6(4*H*)-dione (**22**), Mobile phase: Hexane:MeOH, 90:10; flow rate: 0.5 mL/min.

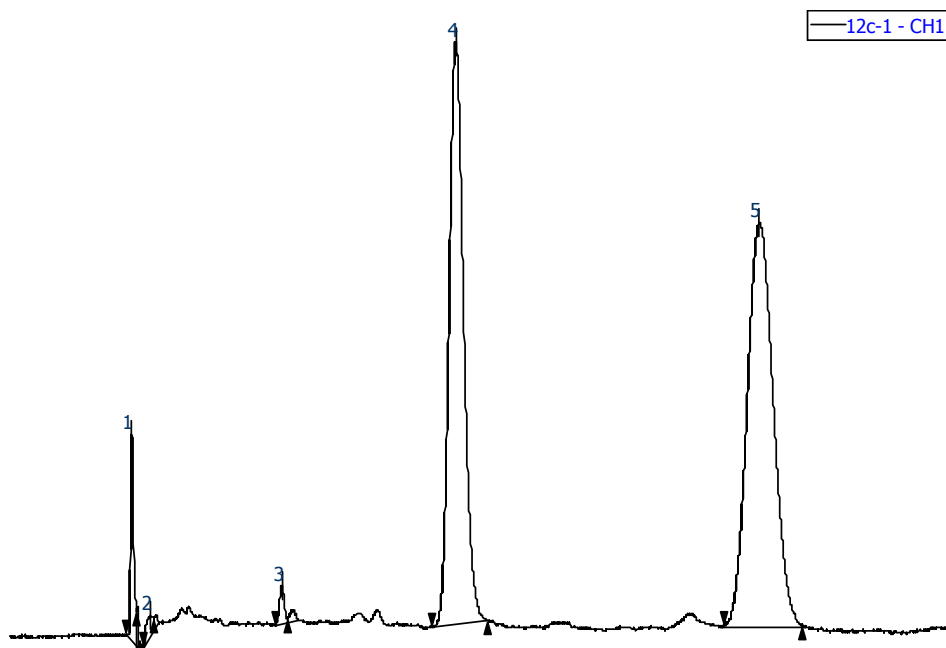


Fig. S35. Chiral analysis of (1*S*,4*R*)-4-((1*H*-indol-3-yl)methyl)-8-chloro-1-isobutyl-1,2-dihydro-6*H*-pyrazino[2,1-*b*]quinazoline-3,6(4*H*)-dione (**23**), Mobile phase: Hexane:MeOH, 90:10; flow rate: 0.5 mL/min.

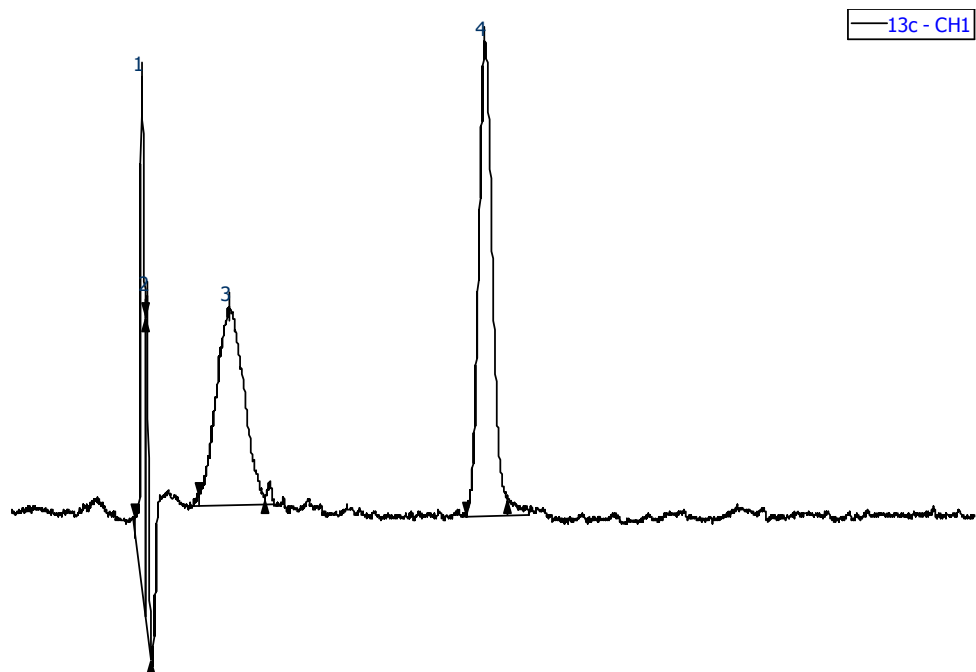


Fig. S36. Chiral analysis of (1*S*,4*R*)-4-((1*H*-indol-3-yl)methyl)-1-((*S*)-sec-butyl)-8-chloro-1,2-dihydro-6*H*-pyrazino[2,1-*b*]quinazoline-3,6(4*H*)-dione (**24**), Mobile phase: Hexane:MeOH, 90:10; flow rate: 0.5 mL/min.

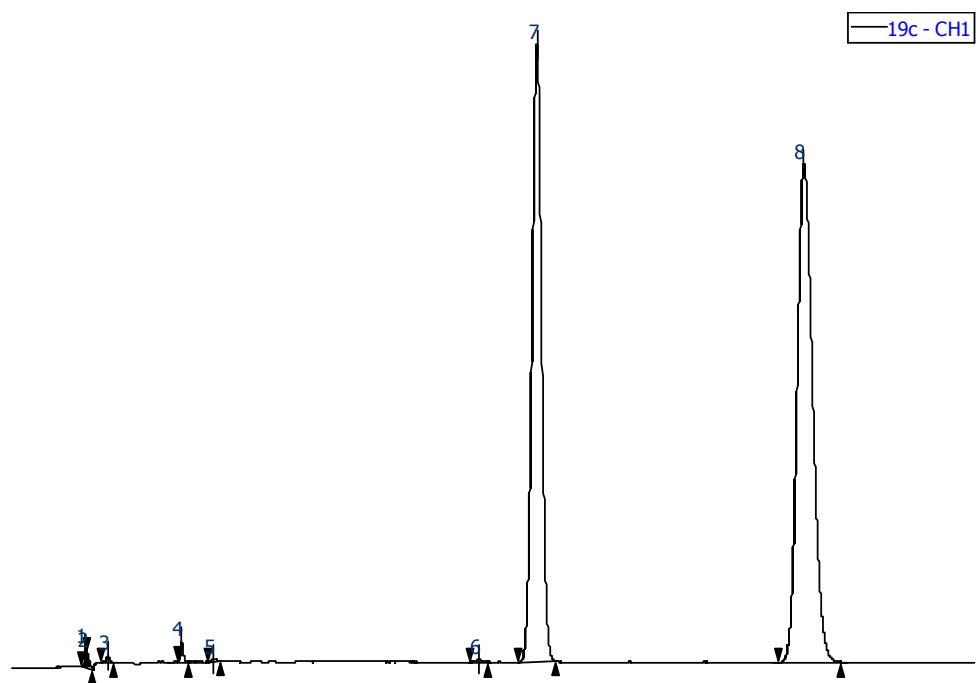


Fig. S37. Chiral analysis of (1*S*,4*R*)-4-((1*H*-indol-3-yl)methyl)-8,10-dichloro-1-isopropyl-1,2-dihydro-6*H*-pyrazino[2,1-*b*]quinazoline-3,6(4*H*)-dione (**25**), Solvent: Hexan:MeOH, 90:10; flow rate: 0.5 mL/min.

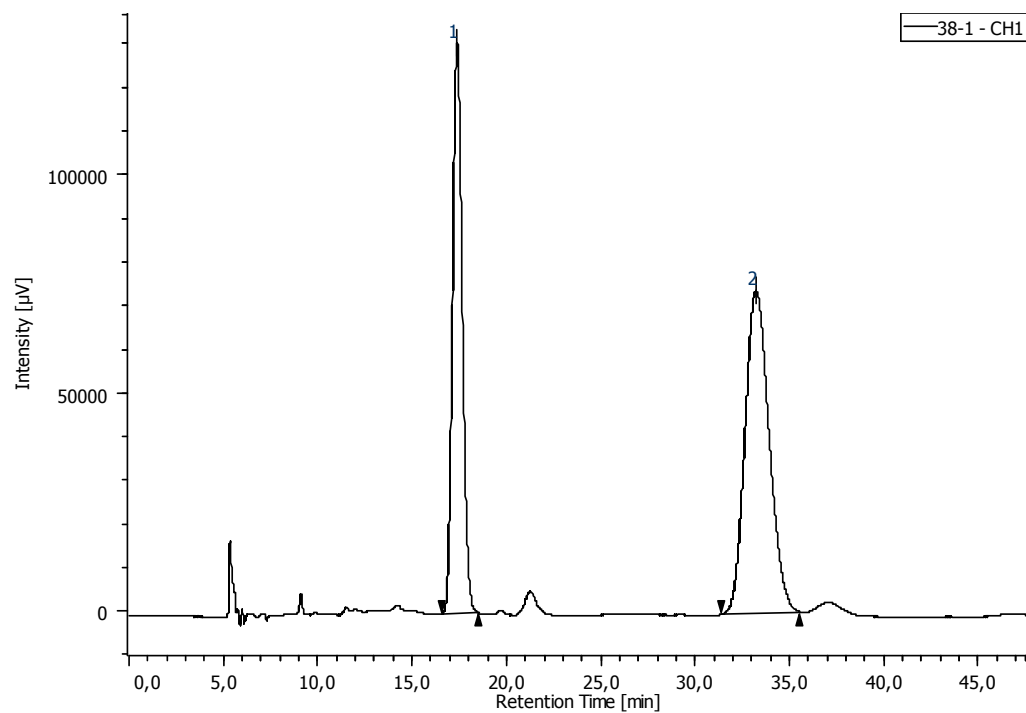


Fig. S38. Chiral analysis of (1*S*,4*R*)-4-((1*H*-indol-3-yl)methyl)-8,10-dichloro-1-isobutyl-1,2-dihydro-6*H*-pyrazino[2,1-*b*]quinazoline-3,6(4*H*)-dione (**26**), Mobile phase: Hexane:MeOH, 90:10; flow rate: 0.5 mL/min.

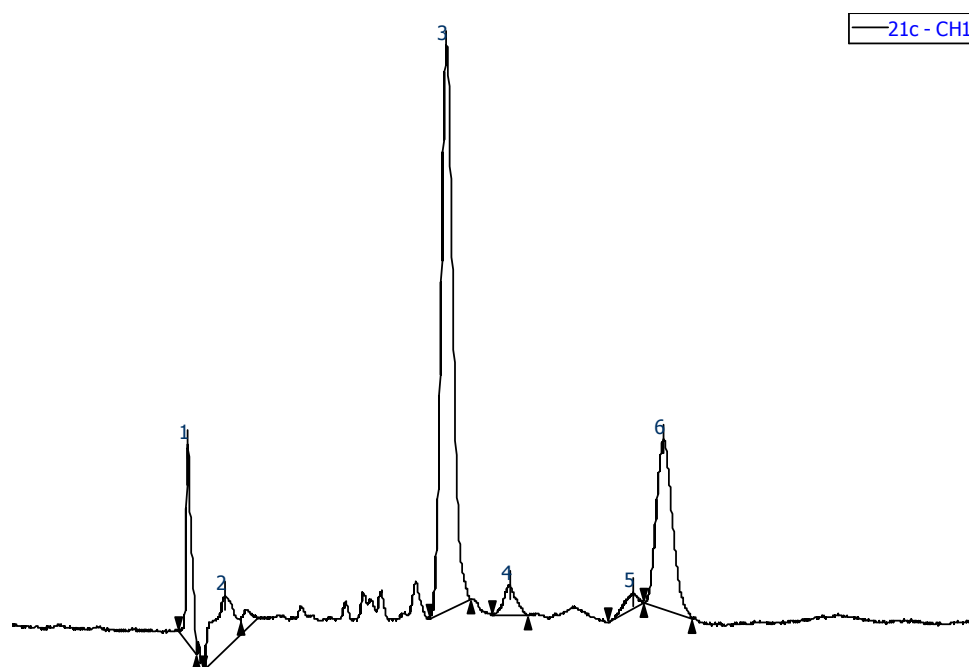


Fig. S39. Chiral analysis of (1*S*,4*R*)-4-((1*H*-indol-3-yl)methyl)-8,10-dichloro-1-((*S*)-sec-butyl)-1,2-dihydro-6*H*-pyrazino[2,1-*b*]quinazoline-3,6(4*H*)-dione (**27**), Mobile phase: Hexane:MeOH, 90:10; flowrate: 0.5 mL/min.

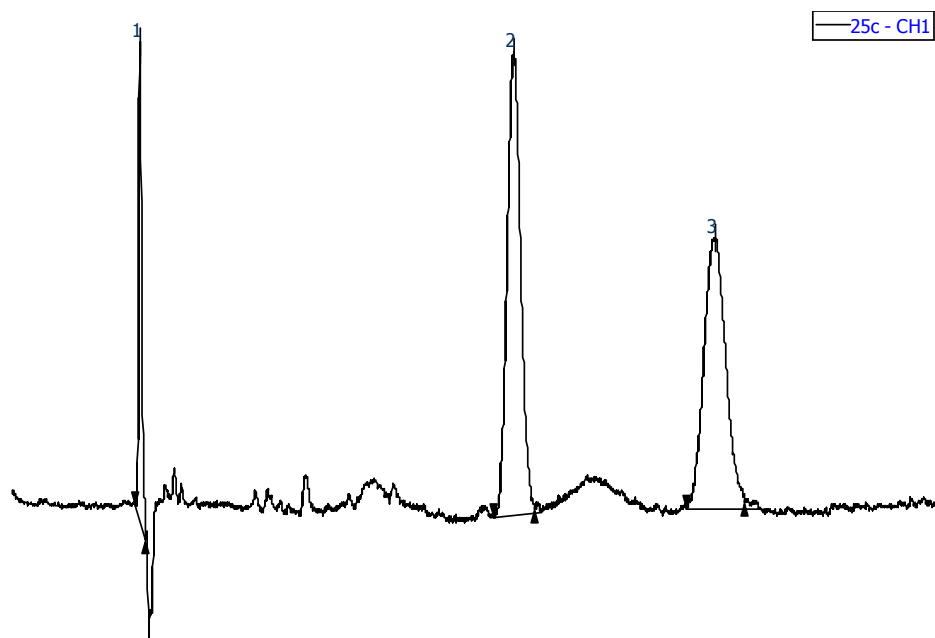


Fig. S40. Chiral analysis of (1*S*,4*R*)-4-((1*H*-indol-3-yl)methyl)-8-iodo-1-isopropyl-1,2-dihydro-6*H*-pyrazino[2,1-*b*]quinazoline-3,6(4*H*)-dione (**28**), Mobile phase: Hexane:MeOH, 90:10; flow rate: 0.5 mL/min.

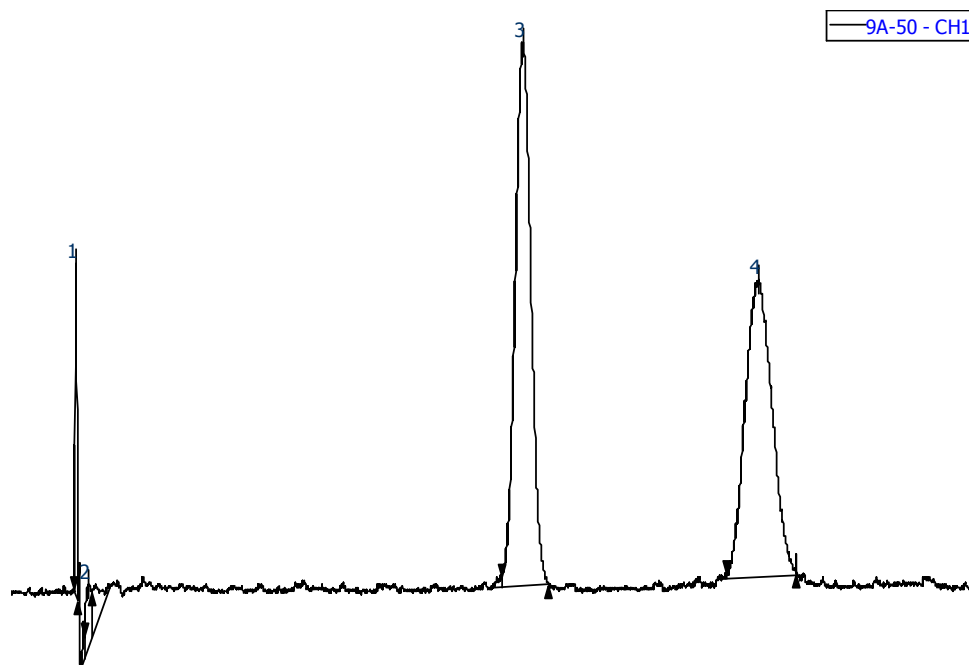


Fig. S41. Chiral analysis of (1*S*,4*R*)-4-((1*H*-indol-3-yl)methyl)-8-bromo-1-isopropyl-1,2-dihydro-6*H*-pyrazino[2,1-*b*]quinazoline-3,6(4*H*)-dione (**29**), Mobile phase: Hexane:MeOH, 90:10; flow rate: 0.5 mL/min.

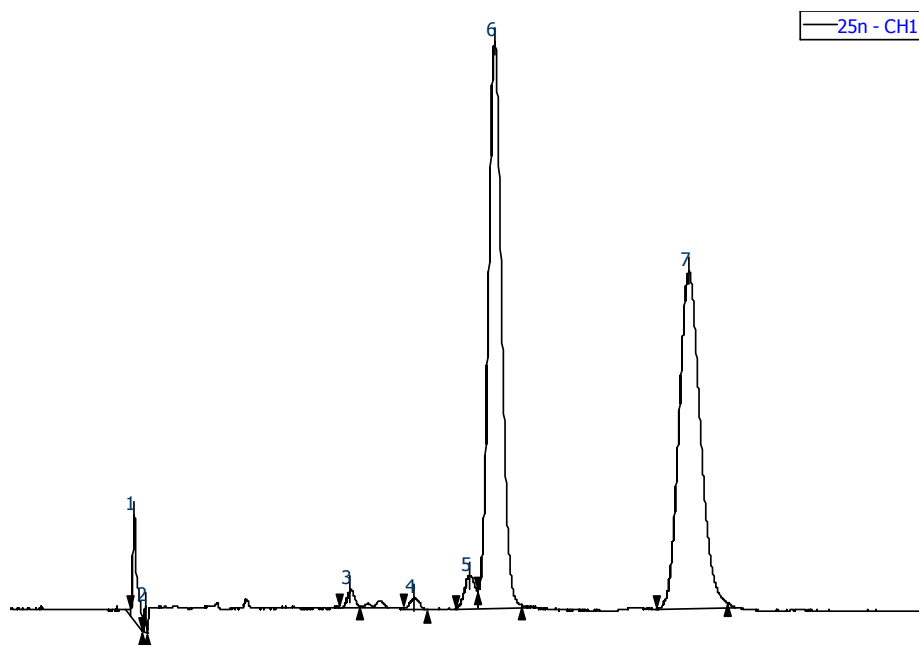


Fig. S42. Chiral analysis of (1*S*,4*R*)-4-((1*H*-indol-3-yl)methyl)-8-iodo-1-isobutyl-1,2-dihydro-6*H*-pyrazino[2,1-*b*]quinazoline-3,6(4*H*)-dione (**30**), Mobile phase: Hexane:MeOH, 90:10; flow rate: 0.5 mL/min.

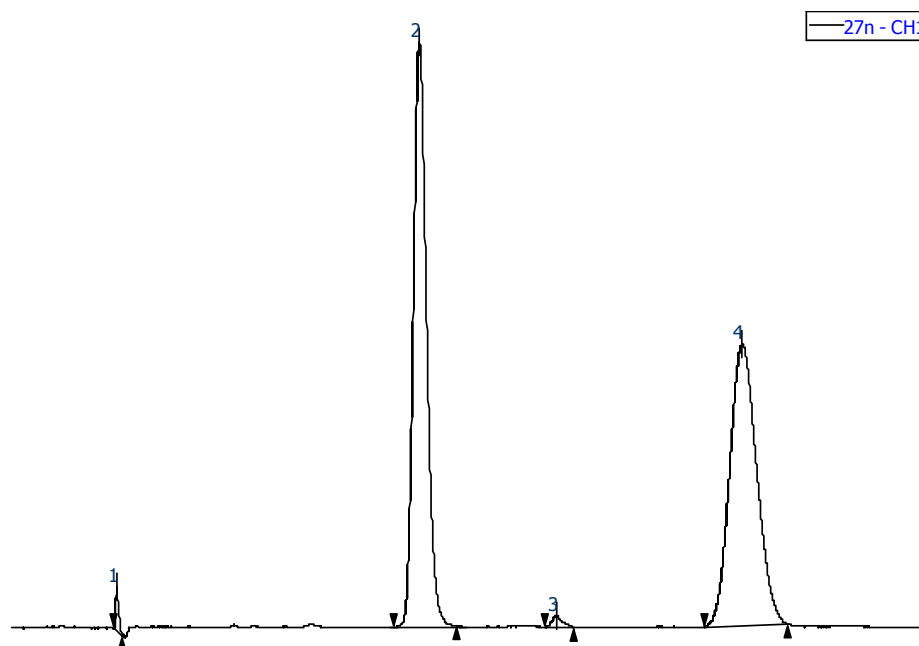


Fig. S43. Chiral analysis of (1*S*,4*R*)-4-((1*H*-indol-3-yl)methyl)-8-bromo-1-isobutyl-1,2-dihydro-6*H*-pyrazino[2,1-*b*]quinazoline-3,6(4*H*)-dione (**31**), Mobile phase: Hexane:MeOH, 90:10; flow rate: 0.5 mL/min.

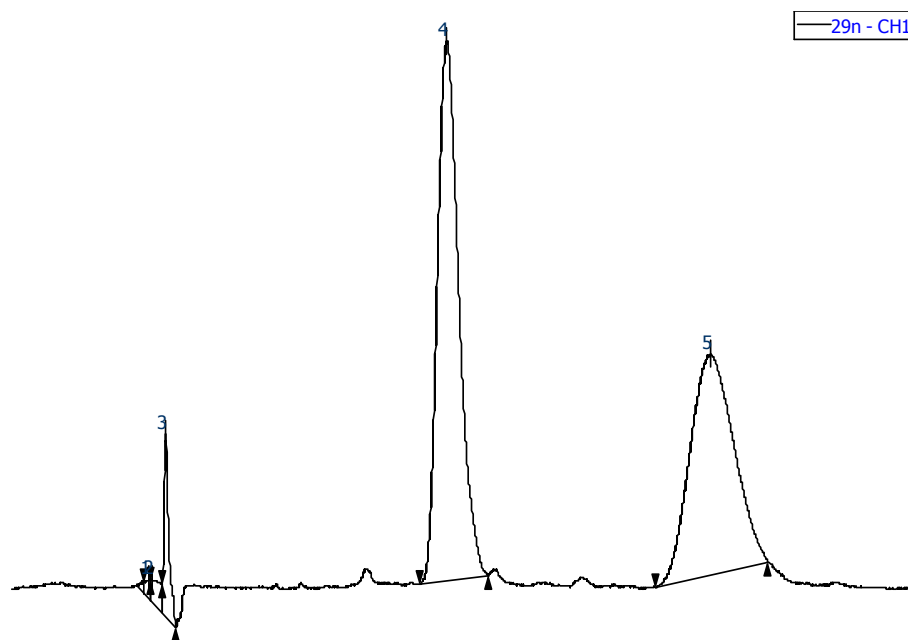


Fig. S44. Chiral analysis of (1*S*,4*R*)-4-((1*H*-indol-3-yl)methyl)-8,10-diiodo-1-isobutyl-1,2-dihydro-6*H*-pyrazino[2,1-*b*]quinazoline-3,6(4*H*)-dione (**32**), Mobile phase: Hexan:MeOH, 90:10; flowrate: 0.5 mL/min.

2.2 Peak purity analyzed on Reversed-Phase HPLC of compounds 22, 23, and 26

The peak purities of most promising compounds were analyzed using reversed-phase liquid chromatography separation employed FortisBIO C18 Column (250 x 4.6 mm, Part number: BIO315-050905), the mobile phase was MeCN/MeOH 50:50, running time: 30 min, minimum wavelength: 210 nm, maximum wavelength: 800 nm. The purity view properties: wavelength range: 225-800 nm, scan threshold: 5 mAU, peak coverage: 95%.

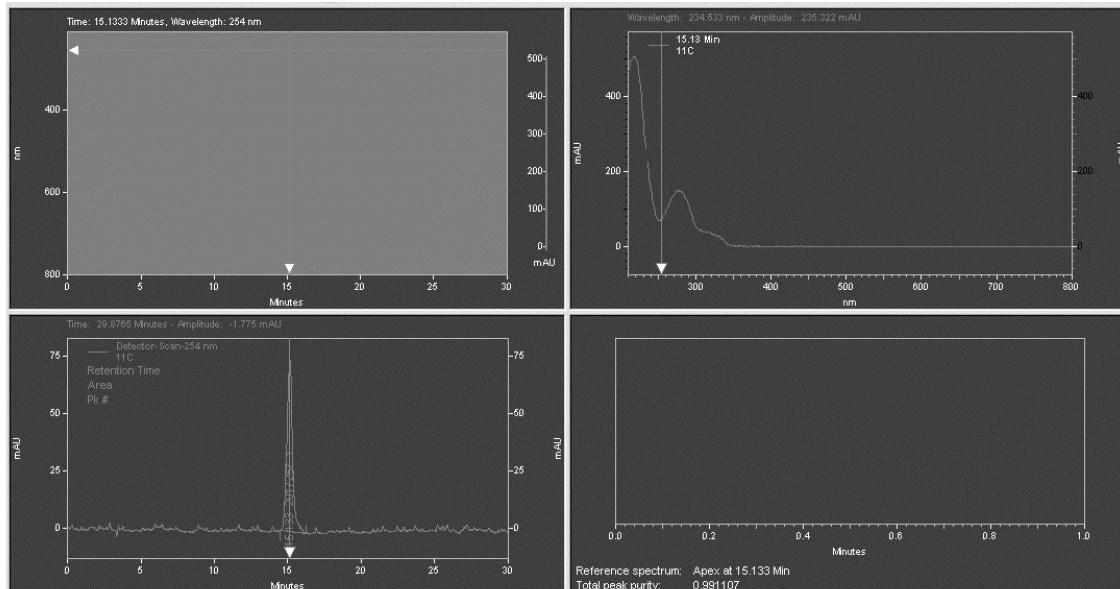


Fig. S45. Peak purity of (1*S*,4*R*)-4-((1*H*-indol-3-yl)methyl)-8-chloro-1-isopropyl-1,2-dihydro-6*H*-pyrazino[2,1-*b*]quinazoline-3,6(4*H*)-dione (**22**).

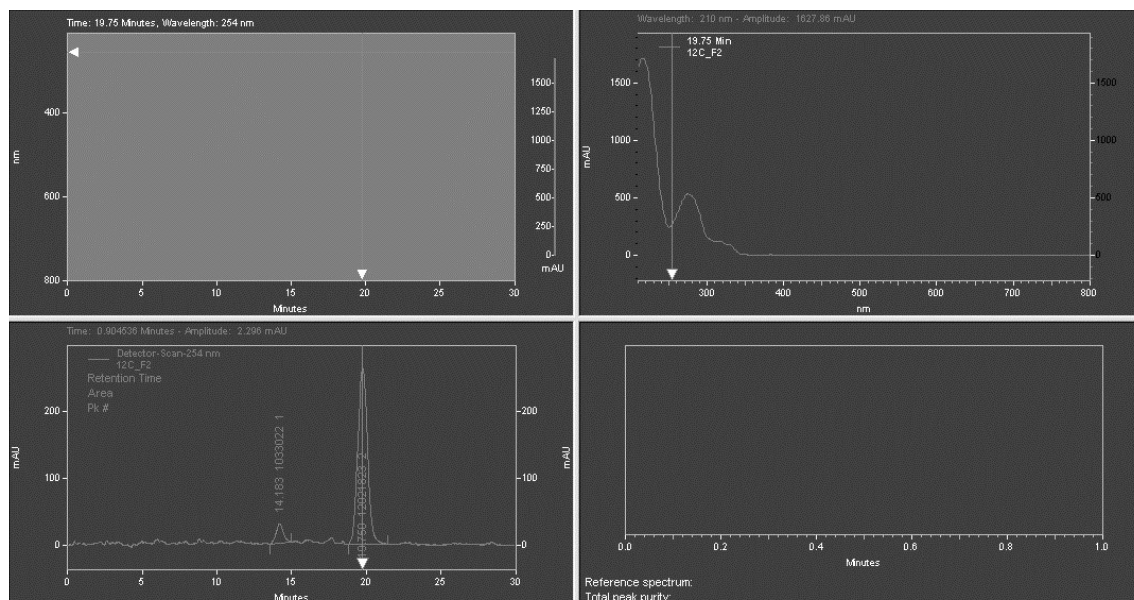


Fig. S46. Peak purity of (1*S*,4*R*)-4-((1*H*-indol-3-yl)methyl)-8-chloro-1-isobutyl-1,2-dihydro-6*H*-pyrazino[2,1-*b*]quinazoline-3,6(4*H*)-dione (**23**).

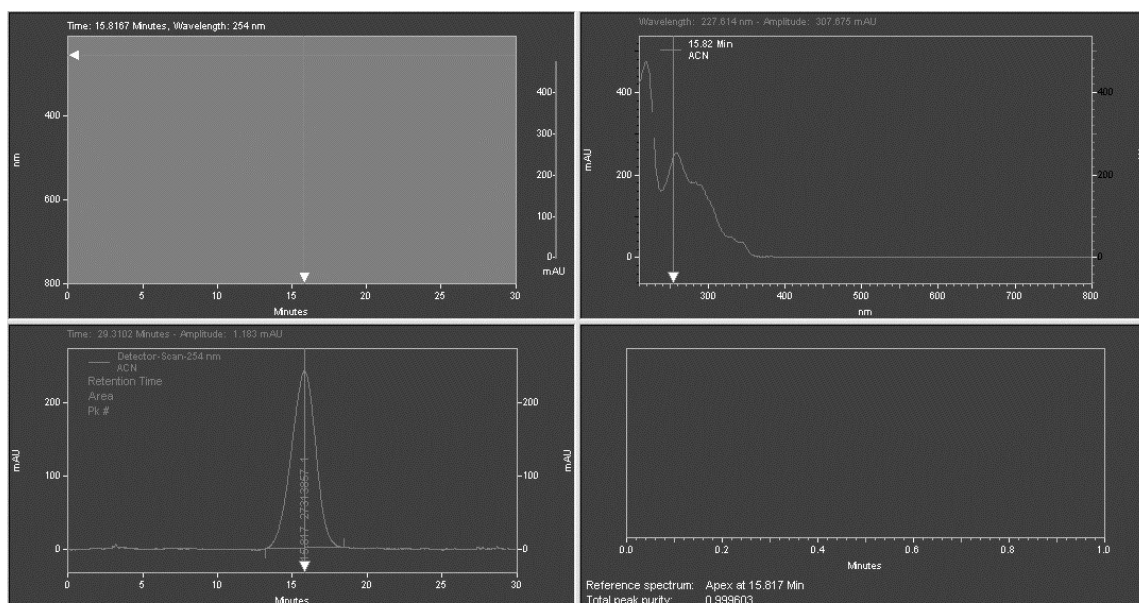


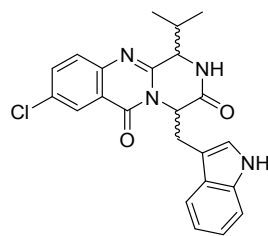
Fig. S47. Peak purity of (1*S*,4*R*)-4-((1*H*-indol-3-yl)methyl)-8,10-dichloro-1-isobutyl-1,2-dihydro-6*H*-pyrazino[2,1-*b*]quinazoline-3,6(4*H*)-dione (**26**).

2.3 Enantioselective liquid chromatography separation of compounds **22**, **23**, and **26**

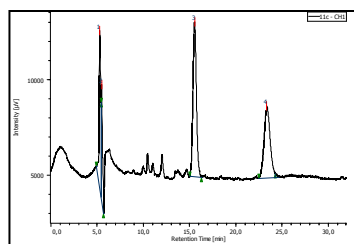
Enantioselective liquid chromatography. In order to evaluate enantioselectivity in vitro activities, such as antibacterial and antifungal, the most promising derivatives **22**, **23**, and **26**, were obtained in milligram scale by semipreparative enantioselective liquid chromatography, employing a tris-3,5-dimethylphenylcarbamate amylose column with multiple injection in a 200 μ L loop. Initial conditions were investigated with analytical Pirkle columns in polar mode [Whelk-O1-S,S (250 \times 4.6 mm) and UV-detection at 245 nm, mobile phase MeOH/MeCN 50:50, flow rate 1.0 mL/min] and polysaccharide based columns (amylose and cellulose) in multimodal conditions. The best analytical conditions [Amylose-1, (250 \times 4.6 mm), mobile phase hexane:EtOH, 90:10, flow rate 0.5 mL/min] presented good separation ($\alpha > 1.2$) and resolution values ($R_s > 8$) for all compounds to allow the scale-up to the preparative mode. The semipreparative separation was optimized by adjusting the sample volume from the analytical method. The optimized mobile phase of analytical system (hexane:EtOH, 90:10) was transferred without any modification to semipreparative mode and 254 was chosen as minimum wavelength absorption. The column diameter was enlarged to a scale-up factor of 3. The flow rate was increase from 0.5 to 2 mL/min, and the retention times were between 15 to 50 min. The loading effect in semipreparative mode was examined by keeping the concentration of the feed solution at the maximum (1.5 mg/mL) and by varying the volume (100 to 200 μ L). The mobile phase composition, chromatograms, and chromatographic parameters (Tables S1 and S2) at analytical and semipreparative scales.

Table S1. Separation performance on the amylose tris-3,5-dimethylphenylcarbamate phase for compounds **22**, **23**, and **26**.

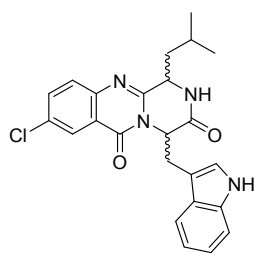
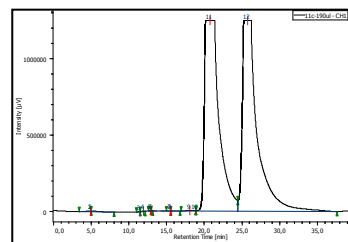
Compounds structure Analytical column [a] Semipreparative column [b]



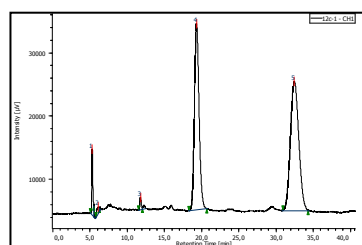
22



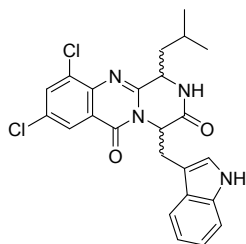
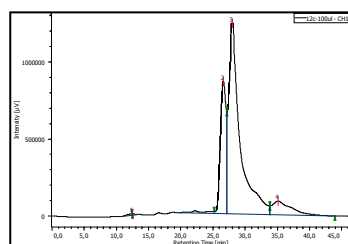
($k_1 = 1.95$, $\alpha = 1.76$ $R_s = 8.43$)



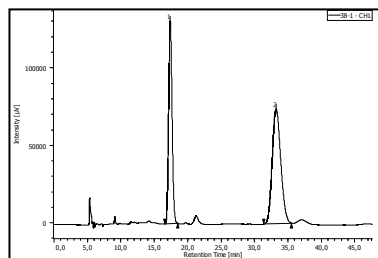
23



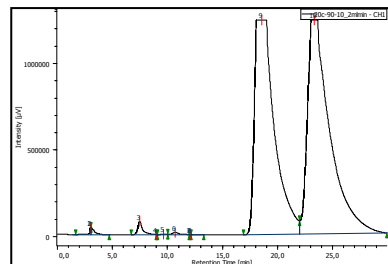
($k_1 = 2.64$, $\alpha = 1.94$ $R_s = 8.15$)



26



($k_1 = 5.60$, $\alpha = 1.75$ $R_s = 11.69$)



[a] Flow rate: 0.5 mL/min, loop 20 μ L, detection: 254 nm, column: Lux[®] 5 μ m Amylose-1, (250 \times 4.6 mm), mobile phase hexane:EtOH, 90:10. k : retention factor, α : enantioselective selectivity, R_s : resolution index. [b] Flow rate: 2 mL/min, loop 200 μ L, loading ca. 1.5 mg/mL in hexane:EtOH (50:50), detection 254 nm, column: amylose tris-3,5-dimethylphenylcarbamate coated with Nucleosil (200 mm \times 7 mm); mobile phase hexane:EtOH, 90:10.

Table S2. Elution order, specific rotation, and enantiomeric excess ($e.r$) of the resolved compound **22**, **23**, and **26** enantiomers.

Enantiomer	Elution order	$[\alpha]_D$ (c) ^a	<i>e.r.</i> (%) ^b
(-)-22	First order	-0.06 (0.08)	>99:1
(+)-22	Second order	+0.04 (0.10)	>99:1
(-)-23	First order	-0.08 (0.05)	>99:1
(+)-23	Second order	+0.22 (0.12)	>99:1
(-)-26	First order	-0.16 (0.03)	97:3
(+)-26	Second order	+0.15 (0.03)	>99:1

[a] Specific rotation in MeOH with c = concentration in g/mL. [b] Enantiomeric ratio (*e.r.*) determined by enantioselective LC described in experimental conditions. Used as an expression of enantiomer purity, this ratio was normalized as a percent.

3. High resolution mass spectra

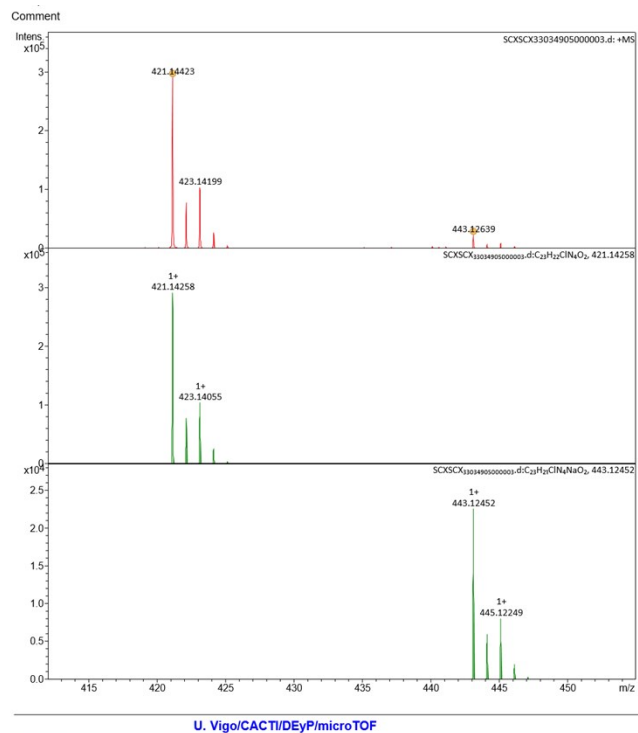


Fig. S48: Mass spectra of (1*S*,4*R*)-4-((1*H*-indol-3-yl)methyl)-8-chloro-1-isopropyl-1,2-dihydro-6*H*-pyrazino[2,1-*b*]quinazoline-3,6(4*H*)-dione (**22**). (20, 300v)

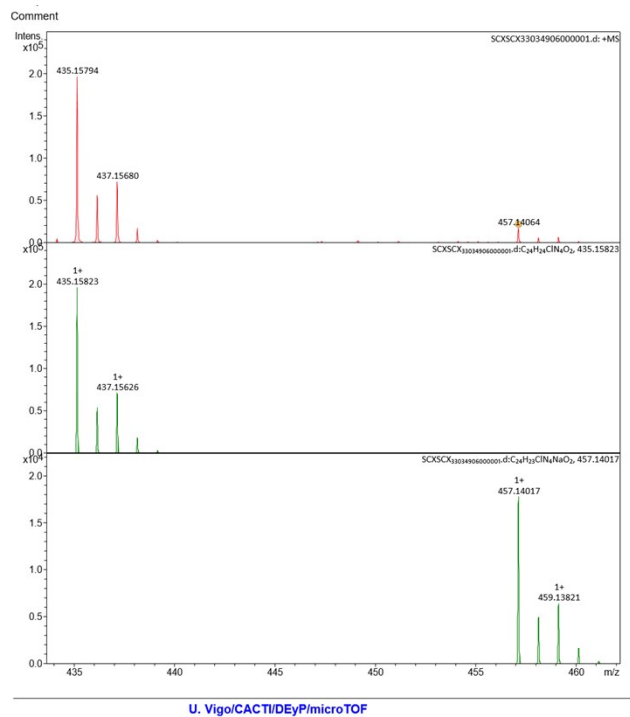


Fig. S49: Mass spectra of (1*S*,4*R*)-4-((1*H*-indol-3-yl)methyl)-8-chloro-1-isobutyl-1,2-dihydro-6*H*-pyrazino[2,1-*b*]quinazoline-3,6(4*H*)-dione (**23**). (20, 300v)

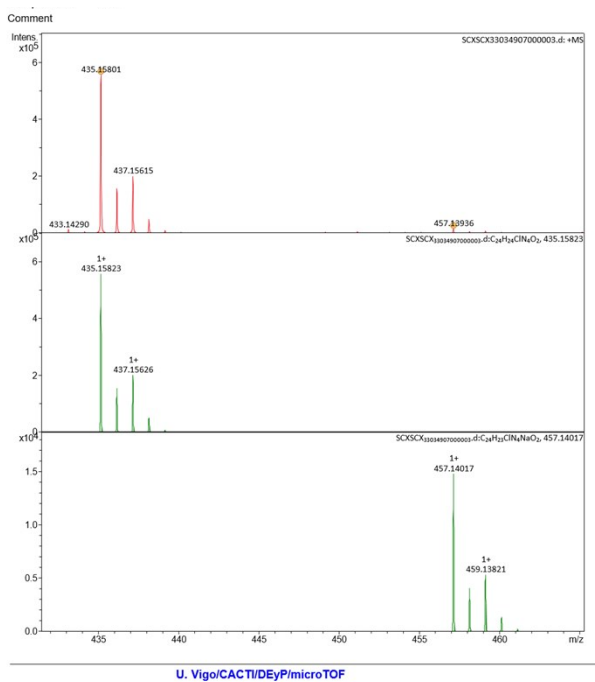


Fig. S50: Mass spectra of (1*S*,4*R*)-4-((1*H*-indol-3-yl)methyl)-1-((*S*)-sec-butyl)-8-chloro-1,2-dihydro-6*H*-pyrazino[2,1-*b*]quinazoline-3,6(4*H*)-dione (**24**). (20, 300v)

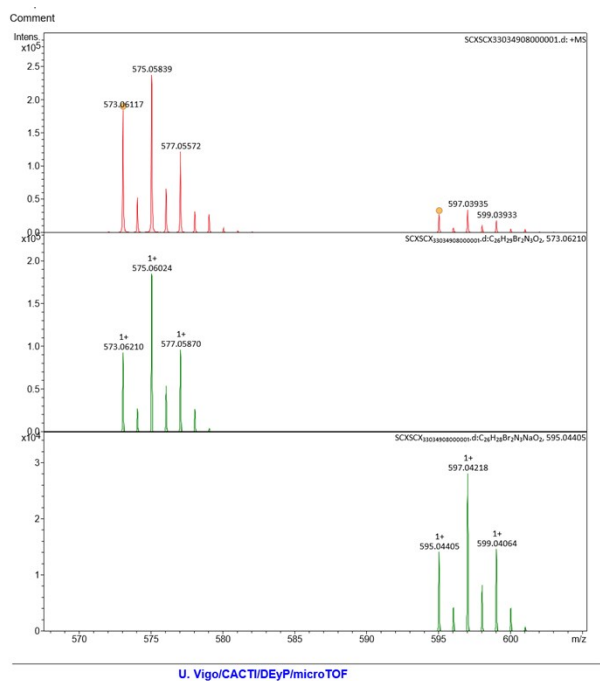


Fig. S51: Mass spectra of (1*S*,4*R*)-4-((1*H*-indol-3-yl)methyl)-8,10-dichloro-1-isopropyl-1,2-dihydro-6*H*-pyrazino[2,1-*b*]quinazoline-3,6(4*H*)-dione (**25**). (20, 300v)

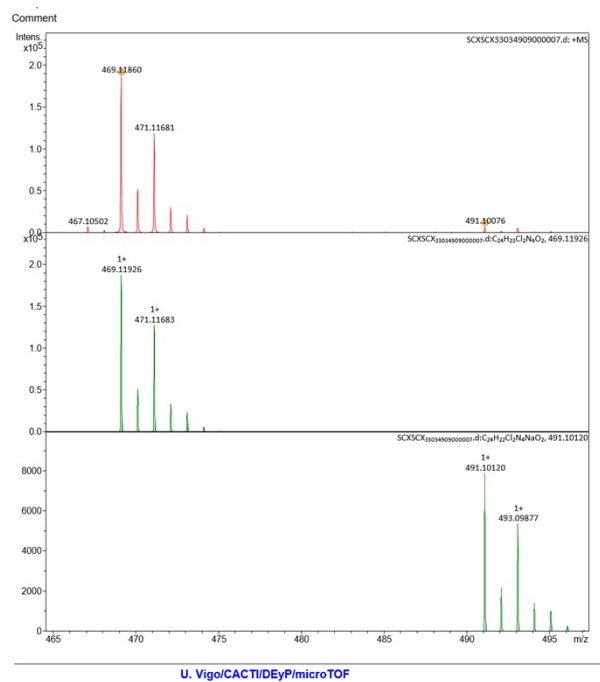


Fig. S52: Mass spectra of (1*S*,4*R*)-4-((1*H*-indol-3-yl)methyl)-8,10-dichloro-1-isobutyl-1,2-dihydro-6*H*-pyrazino[2,1-*b*]quinazoline-3,6(4*H*)-dione (**26**). (20, 300v)

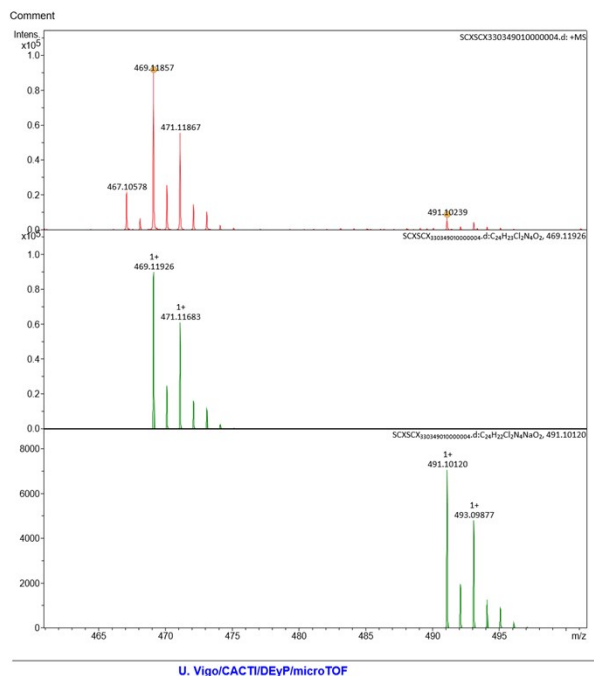


Fig.S53: Mass spectra of (1*S*,4*R*)-4-((1*H*-indol-3-yl)methyl)-1-((*S*)-sec-butyl)-8,10-dichloro-1,2-dihydro-6*H*-pyrazino[2,1-*b*]quinazoline-3,6(4*H*)-dione (**27**). (20, 300v)

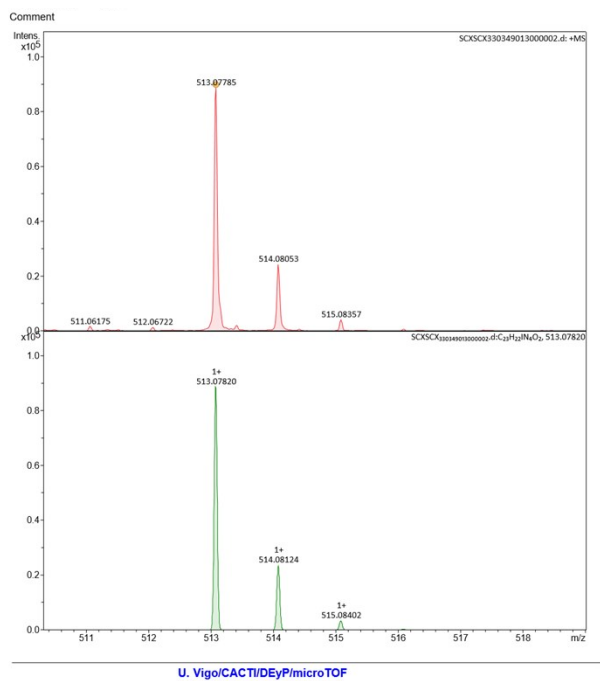


Fig. S54: Mass spectra of (1*S*,4*R*)-4-((1*H*-indol-3-yl)methyl)-8-iodo-1-isopropyl-1,2-dihydro-6*H*-pyrazino[2,1-*b*]quinazoline-3,6(4*H*)-dione (**28**). (20, 300v)

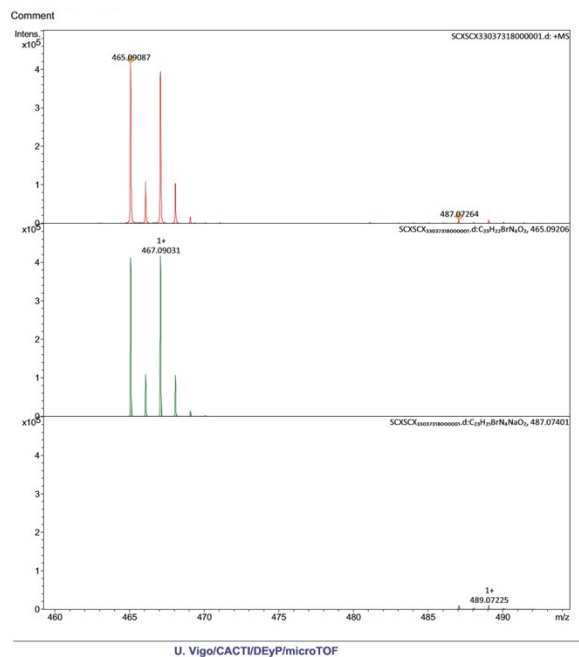


Fig. S55. Mass spectra of (1*S*,4*R*)-4-((1*H*-indol-3-yl)methyl)-8-bromo-1-isopropyl-1,2-dihydro-6*H*-pyrazino[2,1-*b*]quinazoline-3,6(4*H*)-dione (**29**). (20, 300v)

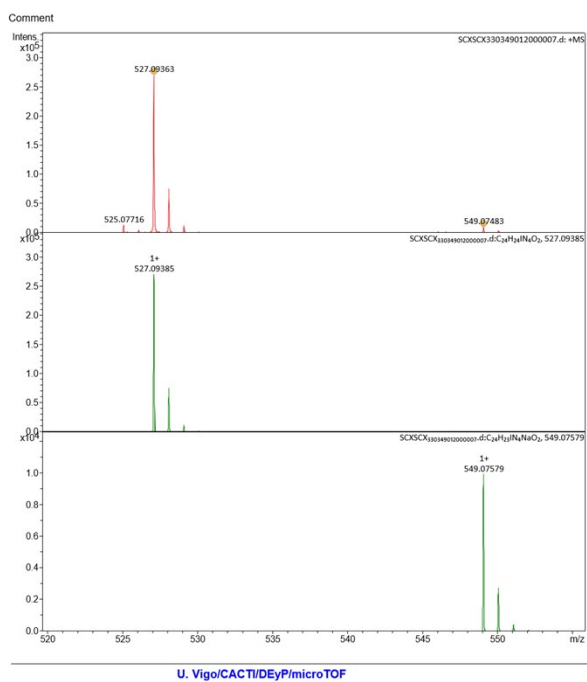


Fig. S56: Mass spectra of (1*S*,4*R*)-4-((1*H*-indol-3-yl)methyl)-8-iodo-1-isobutyl-1,2-dihydro-6*H*-pyrazino[2,1-*b*]quinazoline-3,6(4*H*)-dione (**30**). (20, 300v)

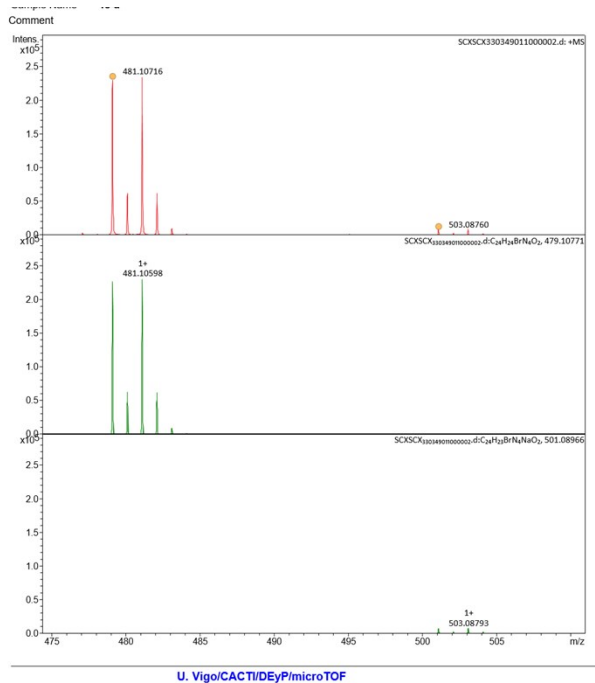


Fig. S57: Mass spectra of (1*S*,4*R*)-4-((1*H*-indol-3-yl)methyl)-8-bromo-1-isobutyl-1,2-dihydro-6*H*-pyrazino[2,1-*b*]quinazoline-3,6(4*H*)-dione (**31**). (20, 300v)

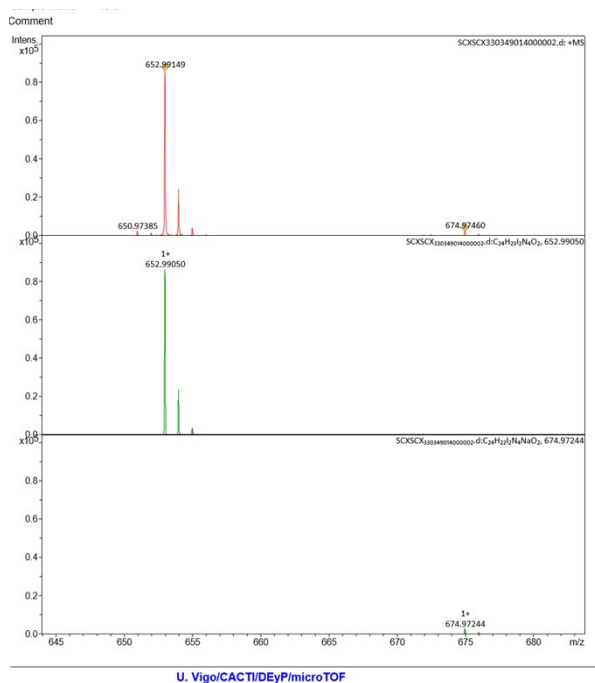


Fig. S58: Mass spectra of (1*S*,4*R*)-4-((1*H*-indol-3-yl)methyl)-8,10-diiodo-1-isobutyl-1,2-dihydro-6*H*-pyrazino[2,1-*b*]quinazoline-3,6(4*H*)-dione (**32**). (20, 300v)

4. Antimicrobial activity

Table S3. Antibacterial activity of quinazolinones **5-32** on Gram-positive and Gram-negative sensitive strains. MIC and MBC are expressed in µg/mL. Inhibition halos are expressed in mm.

	Gram-positive						Gram-negative					
	<i>S. aureus</i> ATCC 29213			<i>E. faecalis</i> ATCC 29212			<i>E. coli</i> ATCC 25922			<i>P. aeruginosa</i> ATCC 27853		
	Halo	MIC	MBC	Halo	MIC	MBC	Halo	MIC	MBC	Halo	MIC	MBC
5	0	>64	ND	0	>64	ND	0	>64	ND	0	>64	ND
6	0	>64	ND	0	>64	ND	0	>64	ND	0	>64	ND
7	0	>64	ND	0	>64	ND	0	>64	ND	0	>64	ND
8	0	>64	ND	0	>64	ND	0	>64	ND	0	>64	ND
9	0	>64	ND	0	>64	ND	0	>64	ND	0	>64	ND
10	0	>64	ND	0	>64	ND	0	>64	ND	0	>64	ND
11	0	>64	ND	0	>64	ND	0	>64	ND	0	>64	ND
12	0	>64	ND	0	>64	ND	0	>64	ND	0	>64	ND
13	0	>64	ND	0	>64	ND	0	>64	ND	0	>64	ND
14	0	>64	ND	0	>64	ND	0	>64	ND	0	>64	ND
15	0	>64	ND	0	>64	ND	0	>64	ND	0	>64	ND
16	0	>64	ND	0	>64	ND	0	>64	ND	0	>64	ND
17	0	>64	ND	0	>64	ND	0	>64	ND	0	>64	ND
18	0	>64	ND	0	>64	ND	0	>64	ND	0	>64	ND
19	0	>64	ND	0	>64	ND	0	>64	ND	0	>64	ND
20	0	>64	ND	0	>64	ND	0	>64	ND	0	>64	ND
21	0	>64	ND	9*	>64	ND	0	>64	ND	0	>64	ND
22	9	>32	> 64	0	>64	>64	0	>64	ND	0	>64	ND
(-)-22	9	>64	ND	0	>64	ND	0	>64	ND	0	>64	ND
(+)-22	9	>64	ND	0	>64	ND	0	>64	ND	0	>64	ND
23	9	>32	> 64	0	>32	>64	0	>64	ND	0	>64	ND
(+)-23	10	>64	ND	0	>64	ND	0	>64	ND	0	>64	ND
24	9	>16	> 64	0	>32	>64	0	>64	ND	0	>64	ND
25	11	>16	> 64	9.5*	>64	ND	8*	>64	ND	0	>64	ND
26	11	>4	> 64	11*	>64	ND	8*	>64	ND	0	>64	ND
(-)-26	11	>4	>64	9	>64	ND	0	>64	ND	0	ND	ND
(+)-26	11	>64	ND	8.5	>64	ND	0	>64	ND	0	ND	ND
27	10	>4	> 64	10*	>64	ND	8*	>64	ND	0	>64	ND
28	9*	> 64	ND	0	>64	ND	8.5*	>64	ND	8.5*	>64	ND
29	0	> 64	ND	0	>64	ND	0	>64	ND	8.5*	>64	ND
30	9.5	>16	> 64	9.5*	>64	ND	8	>64	ND	0	>64	ND
31	9.5	>16	> 64	10*	>64	ND	8	>64	ND	0	>64	ND
32	9	> 64	ND	11*	>64	ND	0	>64	ND	0	>64	ND

MIC, minimum inhibitory concentration; MBC, minimum bactericidal concentration; * halo of partial inhibition; ND, not determined

Table S4. Antibacterial activity of quinazolinones **5-32** on five different bacterial strains. MIC and MBC are expressed in µg/mL. Inhibition halos are expressed in mm.

	<i>S. aureus</i> 66/1 (MRSA)			<i>S. aureus</i> 40/61/24			<i>E. faecalis</i> B3/101 (VRE)			<i>E. coli</i> SA/2			<i>E. faecalis</i> A5/102 (VRE)		
	Hal o	MI C	MB C	Hal o	MI C	MB C	Hal o	MI C	MB C	Hal o	MI C	MB C	Hal o	MI C	MB C
5	0	>64	ND	-	-	-	0	>64	ND	0	>64	ND	-	-	-
6	0	>64	ND	-	-	-	0	>64	ND	0	>64	ND	-	-	-
7	0	>64	ND	-	-	-	0	>64	ND	0	>64	ND	-	-	-
8	0	>64	ND	-	-	-	0	>64	ND	0	>64	ND	-	-	-
9	0	>64	ND	-	-	-	0	>64	ND	0	>64	ND	-	-	-
10	0	>64	ND	-	-	-	0	>64	ND	0	>64	ND	-	-	-
11	0	>64	ND	-	-	-	0	>64	ND	0	>64	ND	-	-	-
12	0	>64	ND	-	-	-	0	>64	ND	0	>64	ND	-	-	-
13	0	>64	ND	-	-	-	7	>64	ND	7	>64	ND	-	-	-
14	0	>64	ND	-	-	-	8	>64	ND	0	>64	ND	-	-	-
15	0	>64	ND	-	-	-	8	>64	ND	0	>64	ND	-	-	-
16	0	>64	ND	-	-	-	8	>64	ND	0	>64	ND	-	-	-
17	0	>64	ND	-	-	-	0	>64	ND	0	>64	ND	-	-	-
18	0	>64	ND	-	-	-	0	>64	ND	0	>64	ND	-	-	-
19	0	>64	ND	-	-	-	0	>64	ND	0	>64	ND	-	-	-
20	0	>64	ND	-	-	-	0	>64	ND	0	>64	ND	-	-	-
21	0	>64	ND	-	-	-	0	>64	ND	0	>64	ND	-	-	-
22	0	>64	ND	ND	64	>64	9	>64	ND	7	ND	ND	ND	>64	>64
(-)-22	9	ND	ND	-	-	-	0	ND	ND	0	ND	ND	-	-	-
(+)-22	9	ND	ND	-	-	-	0	ND	ND	0	ND	ND	-	-	-
23	0	>64	ND	ND	64	>64	8	>64	ND	7	ND	ND	ND	>64	>64
(+)-23	0	ND	ND	-	-	-	0	ND	ND	0	ND	ND	-	-	-
24	9	>64	ND	ND	64	>64	8	>64	ND	7	ND	ND	ND	>64	>64
25	10	>64	ND	ND	>64	ND	0	ND	ND	0	ND	ND	ND	ND	ND
26	10	>8	>64	ND	>8	>64	0	ND	ND	0	ND	ND	ND	ND	ND
(-)-26	0	>4	>64	ND	>4	>64	0	ND	ND	0	ND	ND	ND	ND	ND
(+)-26	0	ND	ND	-	-	-	0	ND	ND	0	ND	ND	-	-	-
27	9.5	>8	>64	ND	>8	>64	0	ND	ND	9	ND	ND	ND	ND	ND
28	10	ND	ND	-	-	-	0	ND	ND	0	ND	ND	-	-	-
29	0	ND	ND	-	-	-	0	ND	ND	0	ND	ND	-	-	-
30	9*	>64	ND	ND	64	>64	0	ND	ND	0	ND	ND	ND	ND	ND
31	10*	>64	ND	ND	>64	ND	0	ND	ND	8.5	ND	ND	ND	ND	ND
32	0	ND	ND	-	-	-	0	ND	ND	0	ND	ND	-	-	-

MIC, minimum inhibitory concentration; MBC, minimum bactericidal concentration; * halo of partial inhibition; ND, not determined

Table S5. Antifungal activity of quinazolines **5-32** against a panel of yeast and filamentous fungi. MIC and MFC are expressed in $\mu\text{g/mL}$.

	<i>C. albicans</i> ATCC 10231		<i>A. fumigatus</i> ATCC 46645		<i>T. rubrum</i> FF5		<i>M. canis</i> FF1		<i>E. floccosum</i> FF9	
	MIC	MFC	MIC	MFC	MIC	MFC	MIC	MFC	MIC	MFC
5	> 128	ND	> 128	ND	> 128	ND	ND	ND	ND	ND
6	> 128	ND	> 128	ND	> 128	ND	ND	ND	ND	ND
7	> 128	ND	> 128	ND	> 128	ND	ND	ND	ND	ND
8	> 128	ND	> 128	ND	> 128	ND	ND	ND	ND	ND
9	> 128	ND	> 128	ND	> 128	ND	ND	ND	ND	ND
10	> 128	ND	> 128	ND	> 128	ND	ND	ND	ND	ND
11	> 128	ND	> 128	ND	> 128	ND	ND	ND	ND	ND
12	> 128	ND	> 128	ND	> 128	ND	ND	ND	ND	ND
13	> 128	ND	> 128	ND	> 128	ND	ND	ND	ND	ND
14	> 128	ND	> 128	ND	> 128	ND	ND	ND	ND	ND
15	> 128	ND	> 128	ND	> 128	ND	ND	ND	ND	ND
16	> 128	ND	> 128	ND	> 128	ND	ND	ND	ND	ND
17	> 128	ND	> 128	ND	> 128	ND	ND	ND	ND	ND
18	> 128	ND	> 128	ND	> 128	ND	ND	ND	ND	ND
19	> 128	ND	> 128	ND	> 128	ND	ND	ND	ND	ND
20	> 128	ND	> 128	ND	> 128	ND	ND	ND	ND	ND
21	> 128	ND	> 128	ND	> 128	ND	ND	ND	ND	ND
22	> 128	ND	> 128	ND	> 128	ND	ND	ND	ND	ND
(-)-22	> 128	ND	> 128	ND	> 128	ND	ND	ND	ND	ND
(+)-22	> 128	ND	> 128	ND	> 128	ND	ND	ND	ND	ND
23	> 128	ND	> 128	ND	> 128	ND	ND	ND	ND	ND
(+)-23	> 128	ND	> 128	ND	> 128	ND	ND	ND	ND	ND
24	> 128	ND	> 128	ND	> 128	ND	ND	ND	ND	ND
25	> 128	ND	> 128	ND	> 128	ND	ND	ND	ND	ND
26	> 128	ND	> 128	ND	128	>128	>128	ND	>128	ND
(-)-26	>128	ND	>128	ND	>128	ND	ND	ND	ND	ND
(+)-26	>128	ND	>128	ND	>128	ND	ND	ND	ND	ND
27	> 128	ND	> 128	ND	> 128	ND	ND	ND	ND	ND
28	> 128	ND	> 128	ND	128	>128	>128	ND	>128	ND
29	> 128	ND	> 128	ND	128	>128	>128	ND	>128	ND
30	> 128	ND	> 128	ND	> 128	ND	ND	ND	ND	ND
31	> 128	ND	> 128	ND	> 128	ND	ND	ND	ND	ND
32	> 128	ND	> 128	ND	> 128	ND	ND	ND	ND	ND

MIC, minimum inhibitory concentration; MFC, minimum fungicidal concentration; ND, not determined

Table S6: Calculated molecular properties of compounds 5-32.

Comp.	MW ^a	LOP ^b	TPSA (Å ²) ^c	nON ^d	nONNH ^e	nrotb ^f	LIP ^g	PK ^h									BIAS ⁱ	WatS ^j
								Glab	BBB	P-gp	CYP1A2	CYP2C19	CYP2C9	CYP2D6	CYP3A4	Log Kp		
5	386.45	3.1	79.78	3	2	3	Yes	High	No	Yes	No	Yes	Yes	Yes	Yes	-6.02 cm/s	0.55	Moderate
6	386.45	3.11	79.78	3	2	3	Yes	High	No	Yes	No	Yes	Yes	Yes	Yes	-6.02 cm/s	0.55	Moderate
7	386.45	3.1	79.78	3	2	3	Yes	High	No	Yes	No	Yes	Yes	Yes	Yes	-6.02 cm/s	0.55	Moderate
8	386.45	3.11	79.78	3	2	3	Yes	High	No	Yes	No	Yes	Yes	Yes	Yes	-6.02 cm/s	0.55	Moderate
9	400.47	3.38	79.78	3	2	4	Yes	High	No	Yes	No	Yes	Yes	Yes	Yes	-5.86 cm/s	0.55	Moderate
10	400.47	3.41	79.78	3	2	4	YEs	High	No	Yes	No	Yes	Yes	Yes	Yes	-5.86 cm/s	0.55	Moderate
11	400.47	3.42	79.78	3	2	4	Yes	High	No	Yes	No	Yes	Yes	Yes	Yes	-5.86 cm/s	0.55	Moderate
12	400.47	3.41	79.78	3	2	4	Yes	High	No	Yes	No	Yes	Yes	Yes	Yes	-5.86 cm/s	0.55	Moderate
13	400.47	3.43	79.78	3	2	4	Yes	High	No	Yes	No	Yes	Yes	Yes	Yes	-5.73 cm/s	0.55	Moderate
14	400.47	2.43	79.78	3	2	4	Yes	High	No	Yes	No	Yes	Yes	Yes	Yes	-5.73 cm/s	0.55	Moderate
15	418.51	3.07	105.08	3	2	5	Yes	High	No	Yes	No	Yes	Yes	Yes	Yes	-6.45 cm/s	0.55	Moderate
16	418.51	3.1	105.08	3	2	5	Yes	High	No	Yes	No	Yes	Yes	Yes	Yes	-6.45 cm/s	0.55	Moderate
17	540.61	4.85	89.01	4	2	7	Yes*	High	No	No	Yes	No	Yes	No	Yes	-5.48 cm/s	0.55	Insoluble
18	540.61	4.83	89.01	4	2	7	Yes*	High	No	No	Yes	No	Yes	No	Yes	-5.48 cm/s	0.55	Insoluble
19	450.49	3.23	100.01	4	3	4	Yes	High	No	Yes	No	Yes	Yes	Yes	No	-6.22 cm/s	0.55	Moderate
20	450.49	3.27	100.01	4	3	4	Yes	High	No	Yes	No	Yes	Yes	Yes	No	-6.22 cm/s	0.55	Moderate
21	358.39	2.55	79.78	3	2	2	Yes	High	No	Yes	No	Yes	Yes	Yes	No	-6.42 cm/s	0.55	Moderate
22	420.89	3.63	79.78	3	2	3	Yes	High	No	Yes	No	Yes	Yes	No	Yes	-5.79 cm/s	0.55	Moderate
23	434.92	3.95	79.78	3	2	4	Yes	High	No	Yes	No	Yes	Yes	No	Yes	-5.62 cm/s	0.55	Poor
24	434.92	3.99	79.78	3	2	4	Yes	High	No	Yes	No	Yes	Yes	No	Yes	-5.49 cm/s	0.55	Poor

Comp.	MW ^a	LOP ^b	TPSA (Å ²) ^c	nON ^d	nONNH ^e	nrotb ^f	LIP ^g	PK ^h									BiAS ⁱ	WatS ^j
								High	No	Yes	No	Yes	Yes	No	Yes	-5.56 cm/s		
25	434.92	4.12	79.78	3	2	3	Yes	High	No	Yes	No	Yes	Yes	No	Yes	-5.56 cm/s	0.55	Poor
26	469.36	4.44	79.78	3	2	4	Yes	High	No	Yes	No	Yes	Yes	No	Yes	-5.39 cm/s	0.55	Poor
27	469.36	4.5	79.78	3	2	4	Yes	High	No	Yes	No	Yes	Yes	No	Yes	-5.26 cm/s	0.55	Poor
28	512.34	3.75	79.78	3	2	3	Yes	High	No	Yes	No	Yes	Yes	No	Yes	-6.33 cm/s	0.55	Poor
29	465.34	3.72	79.78	3	2	3	Yes	High	No	Yes	No	Yes	Yes	No	Yes	-6.01 cm/s	0.55	Poor
30	526.37	4.06	79.78	3	2	4	Yes	High	No	Yes	No	Yes	Yes	No	Yes	-6.17 cm/s	0.55	Poor
31	479.37	4.04	79.78	3	2	4	Yes	High	No	Yes	No	Yes	Yes	No	Yes	-5.85 cm/s	0.55	Poor
32	652.27	4.68	79.78	3	2	4	No	High	No	Yes	No	Yes	Yes	No	No	-6.47 cm/s	0.55	Poor

^aMW =Molecular weight (g/mol)

^b LOP = octanol-water partition coefficient (consensus log P_{o/w})

^c TPSA = Topological polar surface area (Å²)

^d nON = number of hydrogen bond acceptors

^e nONNH = number of hydrogen bond donors

^f nrotb = number of rotatable bonds

^g LIP = Lipinski (* yes with one violation)

^h PK = Pharmacokinetics (Glab = GI absorption, BBB = BBB permeant, P-gp = P-go substrate, CYP = CYP inhibitor, Long Kp (skin permeation))

ⁱ BiAS = Bioavailability score

^j WatS = Water solubility (SILICOS-IT)

*All calculation were obtained from Swiss Institute of Bioinformatic (SwissADME): available at <http://www.swissadme.ch/index.php> (accessed 6th march 2020)